NACA RM L9J13

NACA

RESEARCH MEMORANDUM

WIND-TUNNEL INVESTIGATION AT LOW SPEED TO DETERMINE AERODYNAMIC PROPERTIES OF A JETTISONABLE NOSE SECTION WITH CIRCULAR CROSS SECTION

By Roscoe H. Goodwin

Langley Aeronautical Laboratory
Langley Air Force Base, Va.

Declassified August 23, 1954

NATIONAL ADVISORY COMMITTEE
FOR AERONAUTICS
WASHINGTON

May 19, 1950

NATIONAL ADVISORY COMMITTEE FOR AERONAUTICS

RESEARCH MEMORANDUM

WIND-TUNNEL INVESTIGATION AT LOW SPEED TO DETERMINE AERODYNAMIC PROPERTIES OF A JETTISONABLE NOSE SECTION WITH CIRCULAR CROSS SECTION

By Roscoe H. Goodwin

SUMMARY

The aerodynamic properties of a model of a jettisonable nose section with a circular cross section were determined at low speed from an investigation in the Langley 20-foot free-spinning tunnel. Force and moment measurements were made of the nose section in various positions removed from the fuselage and in a position simulating its final condition of free fall (not under the influence of the fuselage). For each location of the nose, the measurements were made with and without stabilizing fins attached.

The results of the investigation indicated that the aerodynamic characteristics of the nose were greatly affected by proximity to the fuselage. It appears that stabilizing a nose may be necessary to prevent it from turning to about 90° angle of attack, where greatly increased drag would cause high accelerations on a pilot within the nose. The results also indicated that, even for a stabilized nose, it may be necessary to eject the nose forward forcibly in order to prevent high accelerations along the backbone of the pilot.

INTRODUCTION

The National Advisory Committee for Aeronautics is conducting a general investigation of methods of safe pilot escape from high-speed aircraft. One method that has been proposed is to jettison the nose of the airplane at a break-off station immediately rearward of the pilot. It is planned that after the nose has been jettisoned and its speed has decreased, the pilot will leave the nose section and descend with his parachute.

The results of recent experimental investigations (references 1, 2, and 3) have indicated generally similar behavior for dynamically scaled-down models of airplane jettisonable nose sections at low speeds and at low-supersonic speeds. The results of these investigations have indicated that a jettisonable nose section without stabilizing fins tends to turn practically 90° to the wind but that if stabilizing fins are used the nose can be made to continue in a nose-first flight attitude. Furthermore, it appears that a pilot within an unstable jettisonable nose may be subjected to high accelerations due primarily to the increased profile drag of the nose. On the basis of results obtained from tests of a dynamic model of a nose section dropped freely from a fixed portion of the remainder of the model (reference 2), it also was indicated that even a stabilized nose may have to be forcibly ejected forward. The forcible ejection may be necessary in order to prevent large negative longitudinal accelerations on the pilot, which may occur if the nose is merely released and allowed to drop directly down from the fuselage. The results have indicated similar behavior for nose sections generally circular in cross section with and without canopy protuberances. The present low-speed investigation was made in the Langley 20-foot free-spinning tunnel in an attempt to obtain some indications of the aerodynamic characteristics which may affect the path and motion of a nose section during and after separation from the fuselage.

For the investigation, a model of a jettisonable nose such as may be used on a transonic airplane design was used. Force and moment measurements were made with and without stabilizing fins attached to the nose with the nose at various positions forward and below the remaining portion of the fuselage in an attempt to include the path the nose would follow if jettisoned at various airspeeds with various ejection forces. The tests were made for both 0° and 5° angle of attack. To obtain information as to the behavior of the nose when no longer under the aerodynamic influence of the fuselage, force and moment tests were made on the isolated nose with and without fins for angles of attack from 0° to 180°.

SYMBOLS

α angle of attack, degrees

L lift, pounds } data are presented about stability axes

D drag, pounds } data are presented about stability axes

M pitching moment about center of gravity of nose, foot-pounds

q dynamic pressure, pounds per square foot $\left(\frac{1}{2}\rho V^2;\ 5.68\ \text{lb/sq ft for these tests}\right)$

ρ air density, slugs per cubic foot

S wing area (14.3 sq ft, scaled down from a representative transonic airplane design)

V velocity, feet per second

$\bar{c}$ mean aerodynamic chord (2.08 ft, scaled down from a representative transonic airplane design)

C_D drag coefficient (D/qS)

C_L lift coefficient (L/qS)

C_M pitching-moment coefficient $(M/qS\bar{c})$

d diameter of the fuselage at the break-off station, feet

X forward separation of nose section from fuselage, feet

Z downward separation of nose section from fuselage, feet

W weight, pounds

APPARATUS AND TESTS

Model and Balance

All tests were made on a model of a jettisonable nose section with a circular cross section. For the tests which simulated the nose section in the vicinity of the fuselage, a portion of a circular fuselage immediately rearward of the nose was also used. The model used represented approximately $\frac{1}{3.5}$-scale versions of corresponding component parts of a possible transonic airplane design. Photographs of the model mounted for testing are shown in figures 1 and 2. The model was made of $\frac{1}{2}$-inch balsa planking over hardwood bulkheads and stringers. The finished model was covered with tissue paper and doped to achieve a smooth surface. A drawing of the nose and fuselage showing the method of mounting them for tests is presented in figure 3.

As indicated in figure 3, a strain-gage balance was supported on the end of an arm projecting from the fuselage model and was completely enclosed within the nose section. Provision was made for altering the length of the supporting arms so as to obtain various orientations of the nose in front of and below the fuselage. A photograph of the six-component strain-gage balance used to measure the forces and moments is shown as figure 4.

Wind Tunnel and Tests

The Langley 20-foot free-spinning tunnel used for this investigation is a vertical wind tunnel of the annular return type and is capable of attaining speeds of approximately 100 feet per second at the working section. The working section is dodecagonal in cross section with 20 feet between opposite sides.

Lift, drag, and pitching-moment measurements of the nose section were made with and without stabilizing fins with the nose at various positions forward of and below the fuselage for angles of attack of 0° and 5°. For these measurements, the fuselage was set at the same angle of attack as was the nose. For most of the measurements on the finned configuration, the fins were in horizontal and vertical planes through the nose section, as shown in figure 2. For a few of the tests, the fins were displaced 45° from these planes. Lift, drag, and pitching-moment measurements were made of the isolated nose with and without fins for an angle-of-attack range of 0° to 180°.

PRECISION

Several runs were repeated in order to obtain an indication of the precision of the measured results. The maximum difference between results for the original and repeated runs was:

C_D	0.0026
C_L	0.0025
C_M	0.0006

The tunnel-wall effects were considered negligible because of the small size of the model relative to the tunnel.

RESULTS AND DISCUSSION

All force and moment data are presented as nondimensional coefficients based on the wing dimensions (S and $\bar{c}$) scaled down from a representative transonic airplane design.

In the presentation of the results of the force and moment measurements of the nose section in the vicinity of the fuselage, the position of the nose is defined in terms of the nondimensional parameters X/d and Z/d. The data obtained at 0° and 5° angles of attack for the finned nose section when directly ahead of the airplane $\left(\frac{Z}{d} = 0\right)$ are presented as plots of the coefficients against forward separation (X/d) in figures 5 and 6. It can be seen from these figures that there was negligible difference between the results obtained with the fins in horizontal and vertical planes through the nose section and the results obtained with the fins displaced 45° from these planes. Therefore, for the remainder of the tests of the finned nose in the vicinity of the fuselage, the fins were mounted only in the horizontal and vertical planes.

The force and moment data obtained with the model during the tests in which the nose was separated both forward and below the fuselage are presented as plots of C_L, C_D, and C_M against forward separation X/d for various downward separations and also as plots of these coefficients against downward separation Z/d for various forward separations. The C_L data are presented in figures 7 to 10; the C_D data, in figures 11 to 14; and the C_M data, in figures 15 to 18. From these graphs, contour plots of the data were made to provide a convenient over-all picture showing the effects of the fuselage on the aerodynamic properties of the nose section when in various positions relative to the fuselage. These contour plots are shown in figures 19 to 24. As previously indicated, the aerodynamic characteristics of the isolated nose with and without fins were determined for angles of attack from 0° to 180°. These data are presented as plots of the coefficients against angle of attack in figures 25 and 26.

From examination of the C_M contour plots for α of 0° and 5° (figs. 24(a) and 24(b)), it can be seen that for any position of the unfinned nose in the vicinity of the fuselage the variation of C_M against α has an unstable slope. As indicated in figure 26, the unfinned nose out of the influence of the fuselage will likely trim at approximately 90° angle of attack, which is in agreement with data obtained from the previous investigations with dynamic models (references 1, 2, and 3). The results in references 2 and 3 indicate the possibility of large negative accelerations along the pilot's backbone due to the attitude and increased drag of the nose. Reference 4 indicates

the possible danger of such large negative accelerations, although it has been indicated that recent experience by the Air Force points to the possibility that man's tolerance of negative acceleration may be greater than the limits shown in reference 4. If the large accelerations are considered dangerous, it may be necessary to use stabilizing fins on the nose sections.

Based on the data obtained in the present investigation, preliminary calculations of possible paths of the finned nose section jettisoned without forcible ejection have been made. These calculations have indicated that the nose would slide downward from the fuselage through the region of high negative lift shown in the C_L contour plots (figs. 19 and 20). This high-lift region will impose large accelerations on the pilot along his backbone. As an example, assume that a nose section, with fins attached, weighing 800 pounds were jettisoned by an airplane flying 650 feet per second at sea level. From figure 19(a), the nose will be seen to pass through a region near $\frac{Z}{d} = 0.6$ and $\frac{X}{d} = 0$ where the lift coefficient will be approximately -0.08. The acceleration a in g's due to lift can be calculated from the relation:

$$a = \frac{C_L \frac{1}{2}\rho V^2 S}{W}$$

For this example, $C_L = -0.08$, $\rho = 0.002378$ slugs per cubic foot, $V = 650$ feet per second, $S = 175$ square feet, $W = 800$ pounds, and the acceleration is:

$$a = \frac{-0.08\left(\frac{1}{2}\right)0.002378(650)^2 175}{800} = -8.8 \text{ g's}$$

This result is in agreement with the results from an investigation with small dynamic models (reference 2). If the large negative acceleration is considered dangerous to a pilot, it may be necessary to eliminate it by forcibly ejecting the nose forward of the remainder of the airplane.

The C_L and C_D contour charts indicate that when a nose is forcibly ejected it may enter regions where the aerodynamic influence of the fuselage will cause increases in the lift and drag forces on the nose, and these increased forces may tend to prevent continued separation between the two bodies. Another factor which may be adverse to continued separation was noted in the results of the experimental investigation of reference 5, wherein shielding by the nose during the initial phase of separation prevented rapid deceleration of the rear body. In this reference, however, it was shown that for a given design, sufficient force could be applied to allow for continued separation.

From examination of the C_M contour plots for α of 0° and 5° (figs. 23(a) and (b)), it can be seen that for any position of the finned nose in the vicinity of the fuselage the variation of C_M against α has a stable slope and indicates some positive or negative trim angle. Inasmuch as the data for the isolated nose (fig. 26) indicate a trim angle of 0°, it appears that the proximity of the fuselage had an effect on the static trim point of the nose. However, this is not considered to be of serious consequence as regards the problem of successful pilot escape by nose jettisoning because forcible forward ejection would undoubtedly move the nose rapidly forward of the region where the fuselage would appreciably influence the trim angles of the nose in a manner similar to that indicated in reference 5.

CONCLUDING REMARKS

The results of a low-speed investigation in the Langley 20-foot free-spinning tunnel indicated that the aerodynamic characteristics of a jettisonable nose section are affected by proximity to the fuselage. It appears that it may be necessary to stabilize a nose to prevent it from turning to about 90° angle of attack, where increased drag would cause high accelerations on a pilot within the nose. The results also indicate that, even for a stabilized nose, it may be necessary to eject the nose forward forcibly in order to prevent high accelerations along the backbone of the pilot.

Langley Aeronautical Laboratory
National Advisory Committee for Aeronautics
Langley Air Force Base, Va.

REFERENCES

1. Scher, Stanley H.: An Empirical Criterion for Fin Stabilizing Jettisonable Nose Sections of Airplanes. NACA RM L9I28, 1949.

2. Scher, Stanley H., and Gale, Lawrence J.: Motion of a Transonic Airplane Nose Section When Jettisoned as Determined from Wind-Tunnel Investigations on a $\frac{1}{25}$-Scale Model. NACA RM L9L08a, 1950.

3. Gale, Lawrence J.: The Path and Motion of Scale Models of Jettisonable Nose Sections at Supersonic Speeds as Determined from an Investigation in the Langley Free-Flight Apparatus. NACA RM L9J13a, 1950.

4. Lombard, Charles F.: How Much Force Can Body Withstand? Aviation Week, vol. 50, no. 3, Jan. 17, 1949, pp. 20-28.

5. Lundstrom, Reginald R., and O'Kelly, Burke R.: Flight Investigation of the Jettisonable-Nose Method of Pilot Escape Using Rocket-Propelled Models. NACA RM L9D11, 1949.

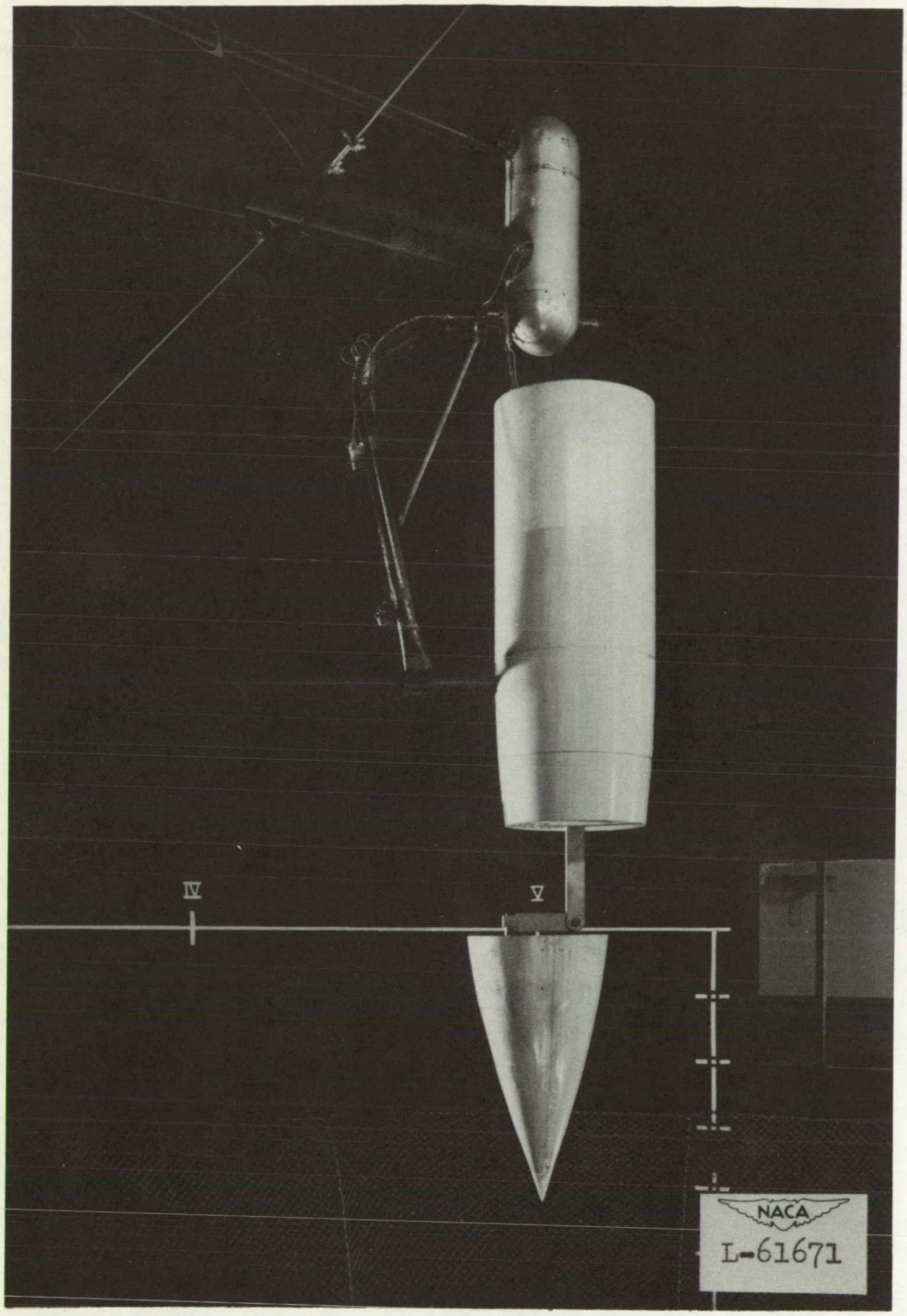

Figure 1.- Assembly used to obtain force and moment measurements of the $\frac{1}{3.5}$-scale nose section in the vicinity of the fuselage. Nose shown without stabilizing fins. $\alpha = 0^{\circ}$.

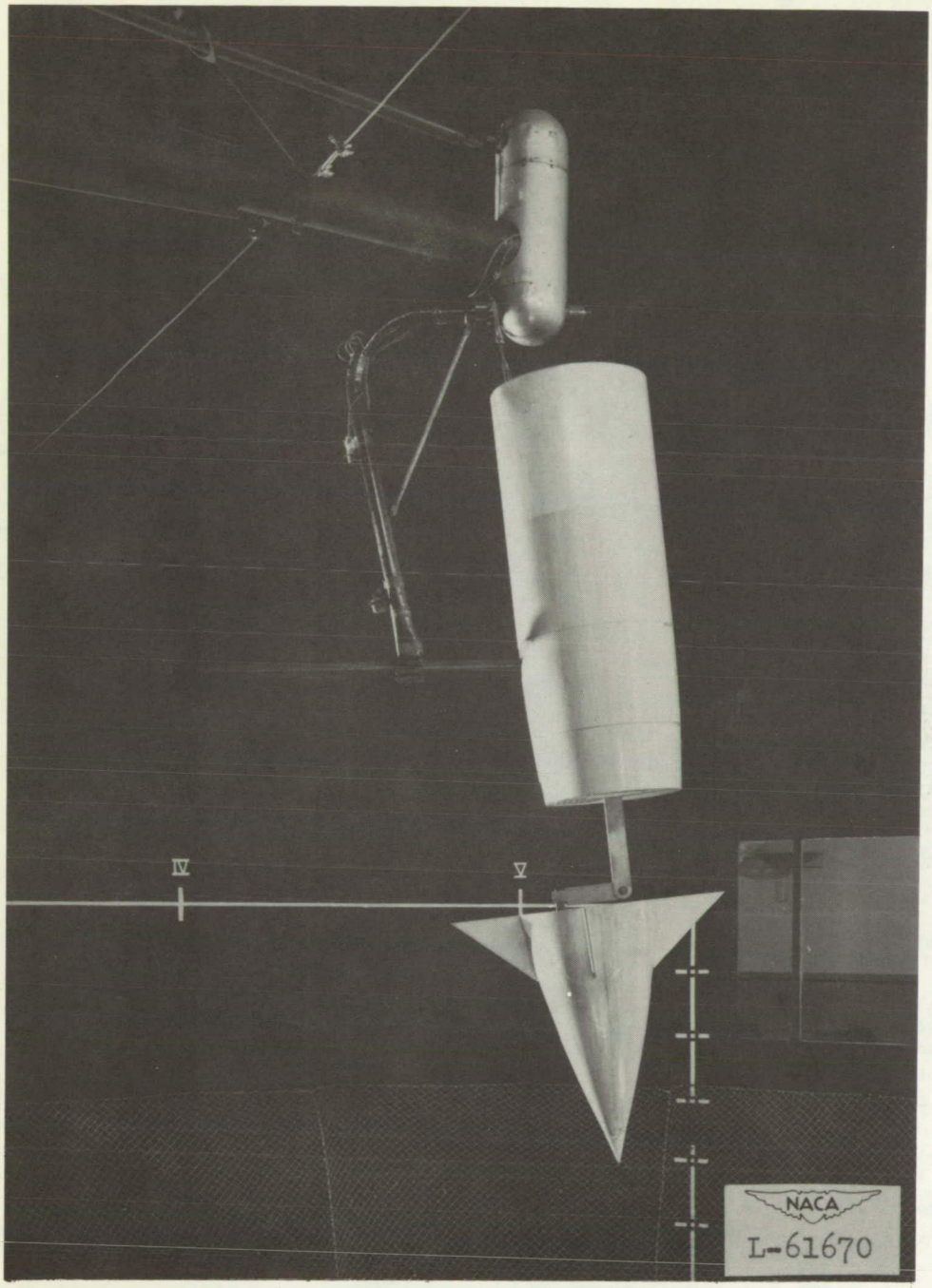

Figure 2.- Assembly used to obtain force and moment measurements of the $\frac{1}{3.5}$-scale nose section in the vicinity of the fuselage. Nose shown with stabilizing fins. $\alpha = 5^{\circ}$.

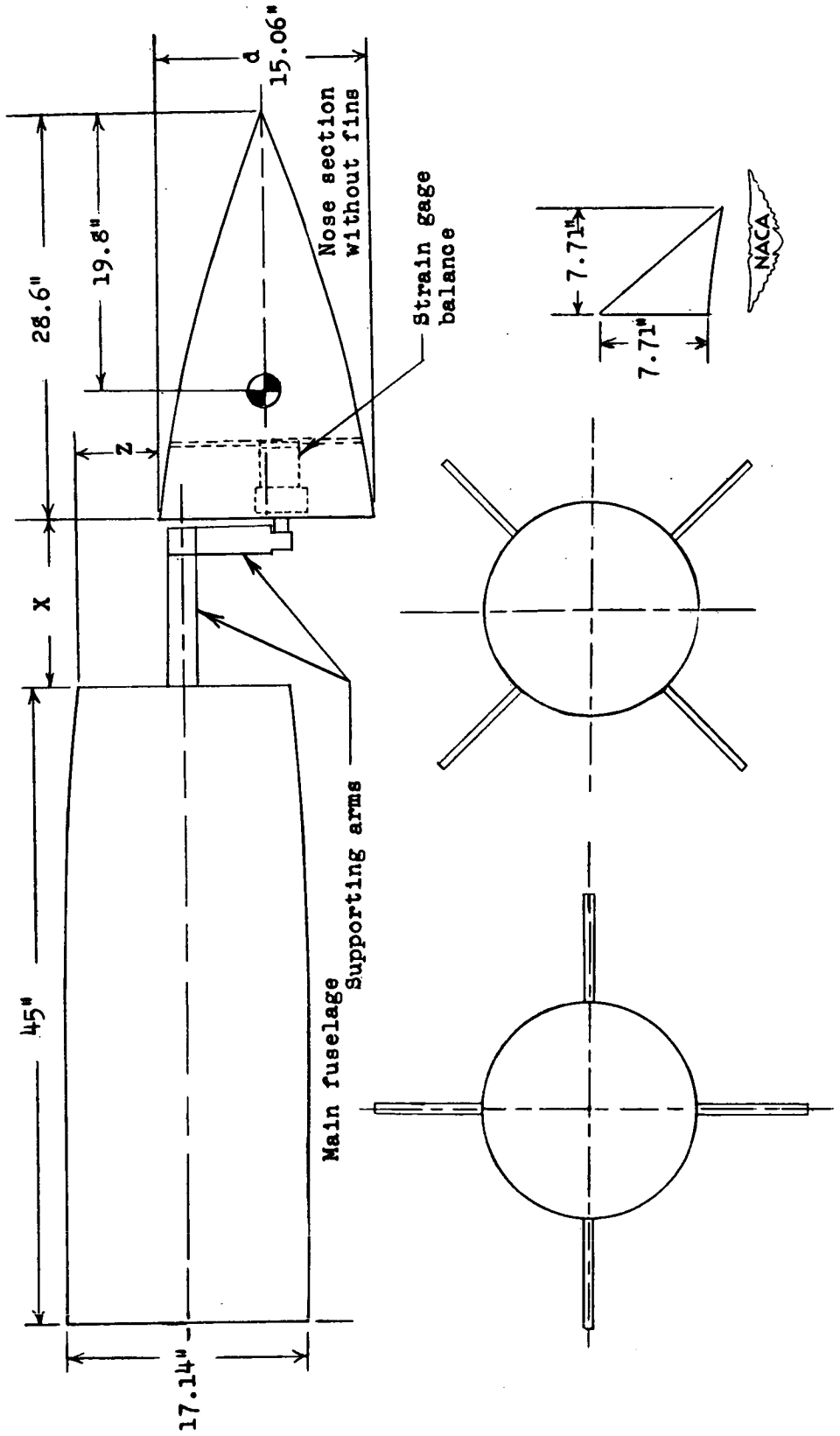

Figure 3.- Sketch of the model of the partial fuselage and jettisonable nose section used in the investigation.

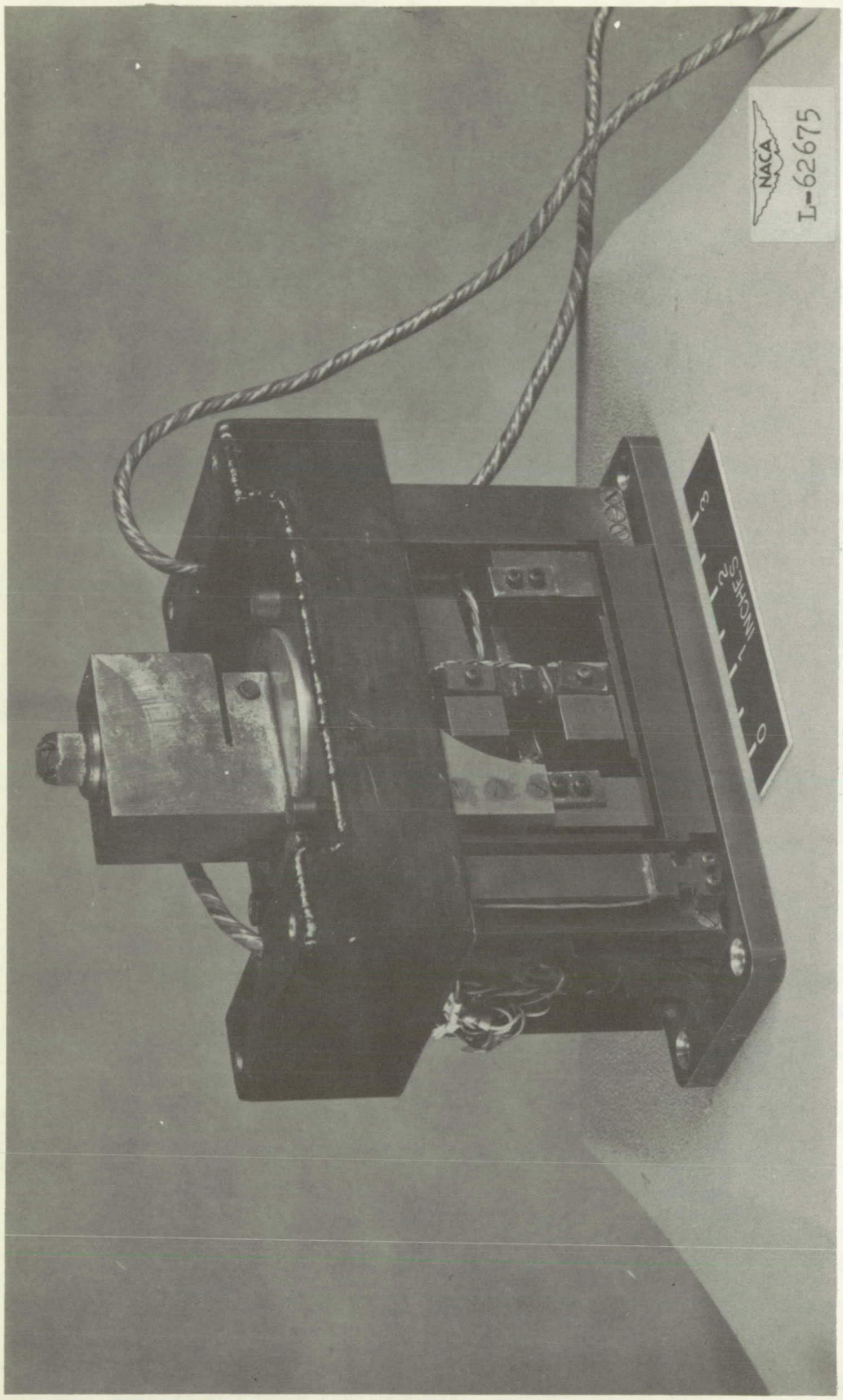

Figure 4.- Six-component strain-gage balance used to obtain force and moment measurements of the model of the jettisonable nose section.

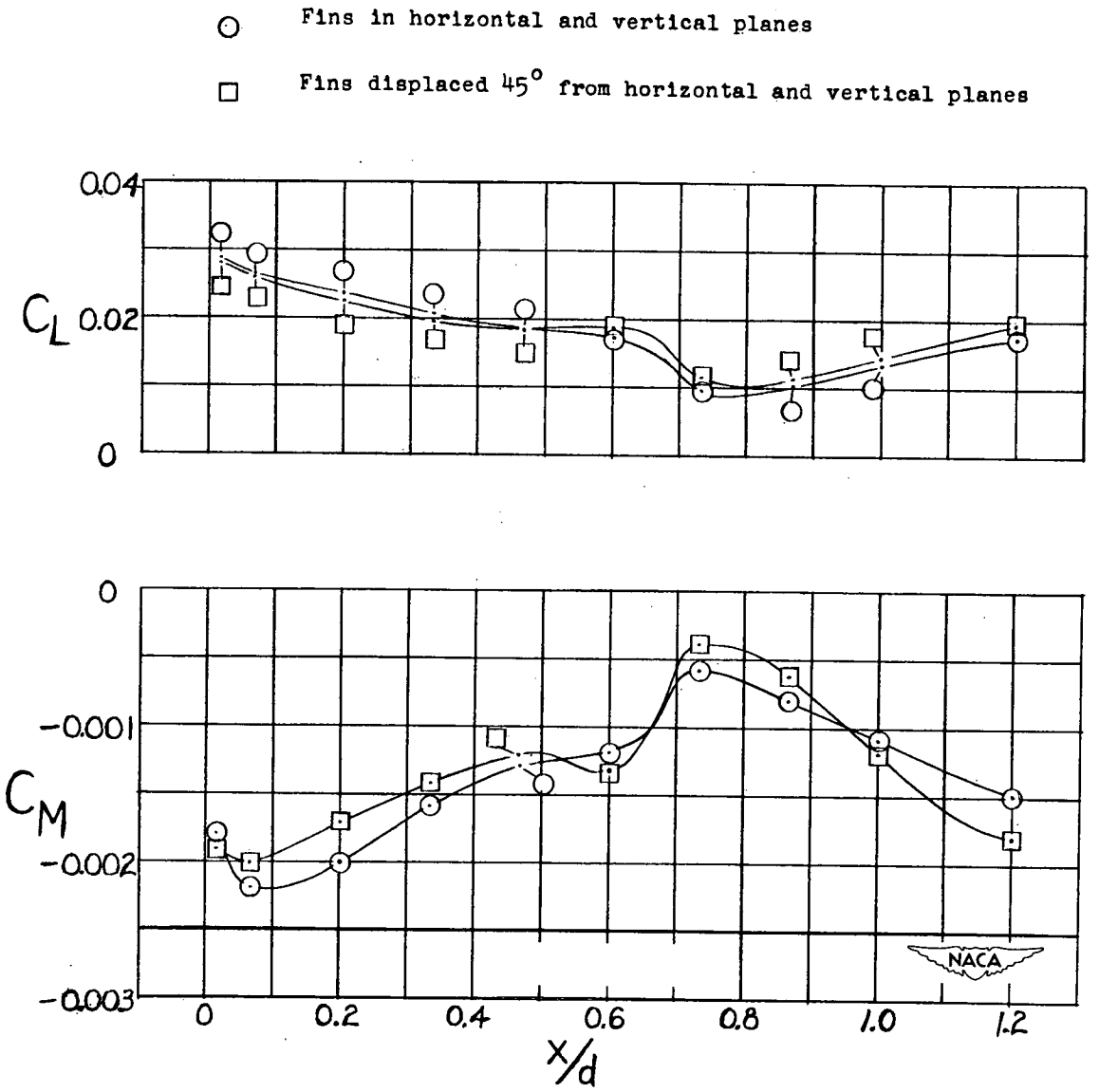

Figure 5.- Comparison of C_L and C_M against X/d with fins in alternate locations. $\frac{Z}{d} = 0$; $\alpha = 5^{\circ}$.

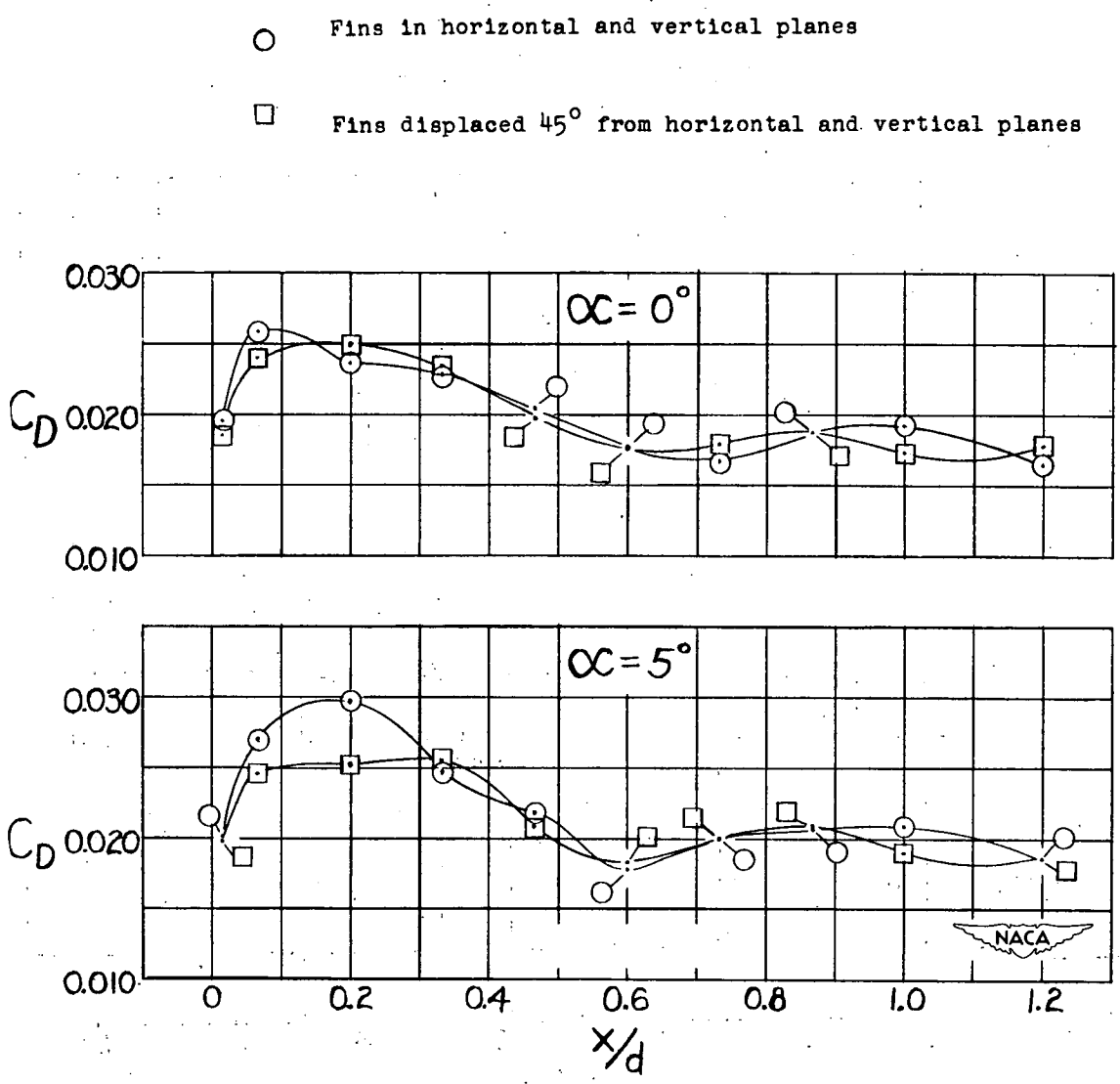

Figure 6.- Comparison of C_D against X/d with fins in alternate locations. $\frac{Z}{d} = 0$.

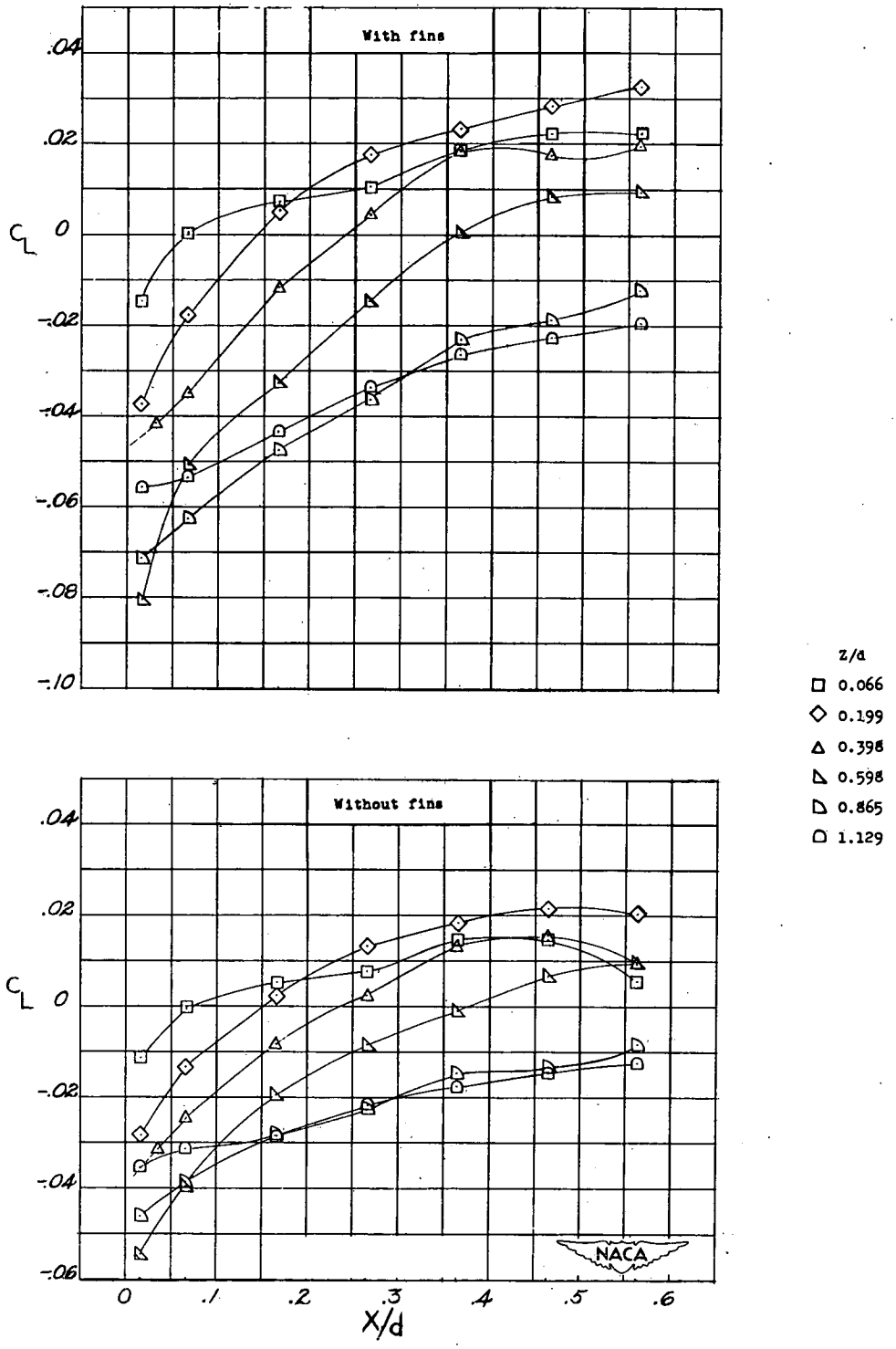

Figure 7.- Variation of C_L with X/d for various Z/d's at $\alpha = 0^{\circ}$ for model with and without fins.

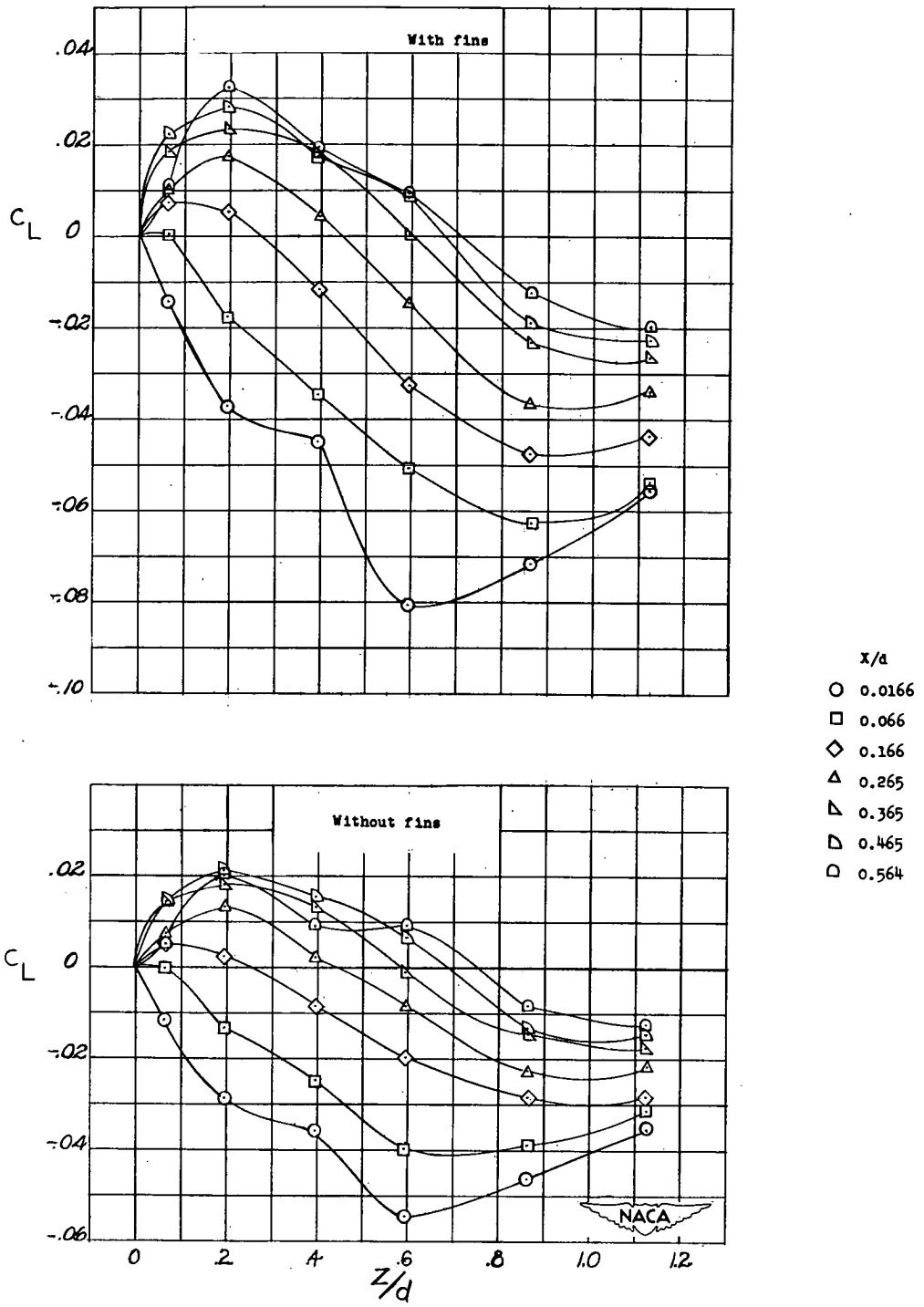

Figure 8.- Variation of C_L with Z/d for various X/d's at $\alpha = 0^\circ$ for model with and without fins.

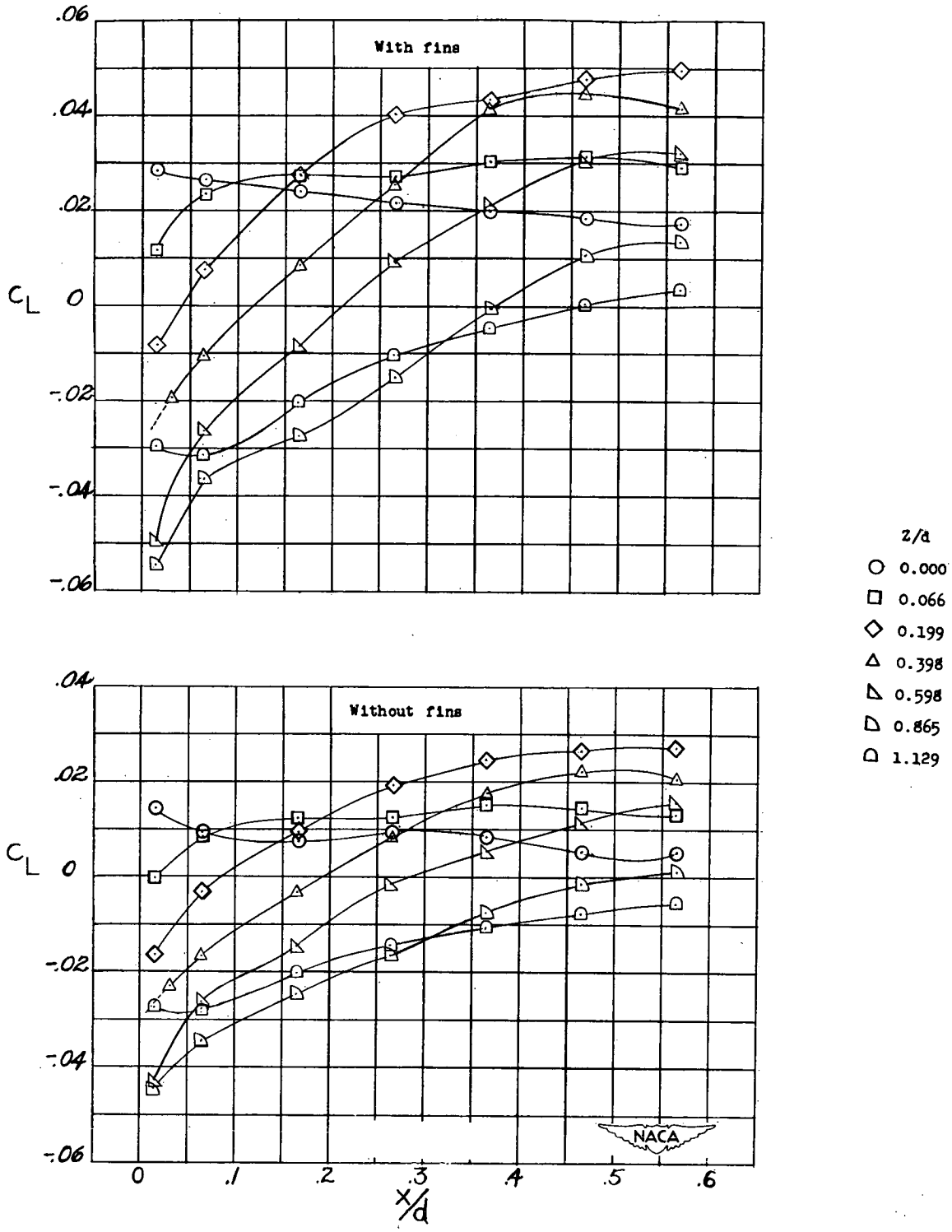

Figure 9.- Variation of C_L with X/d for various Z/d's at $\alpha = 5^{\circ}$ for model with and without fins.

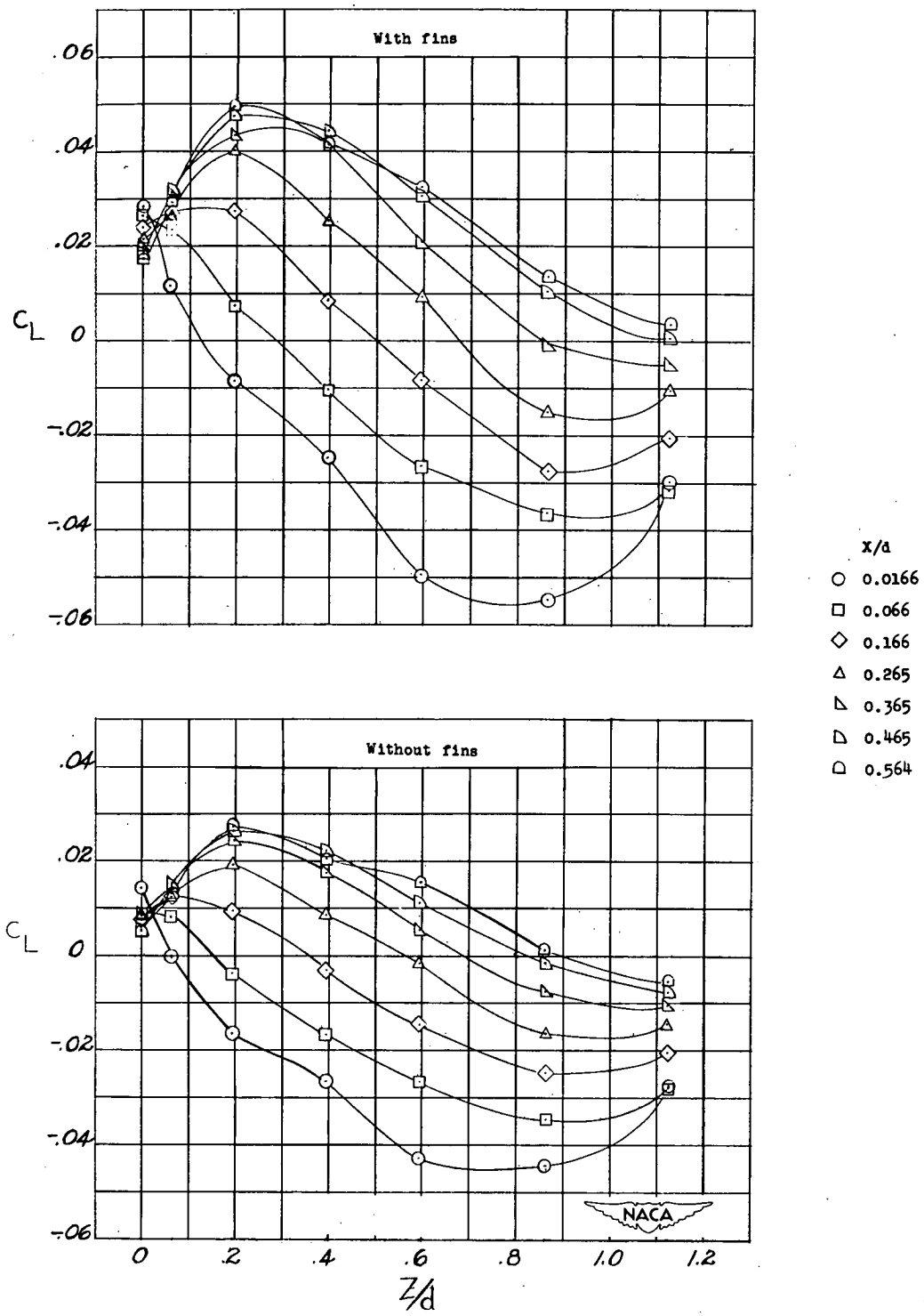

Figure 10.- Variation of C_L with Z/d for various X/d's at $\alpha = 5^{\circ}$ for model with and without fins.

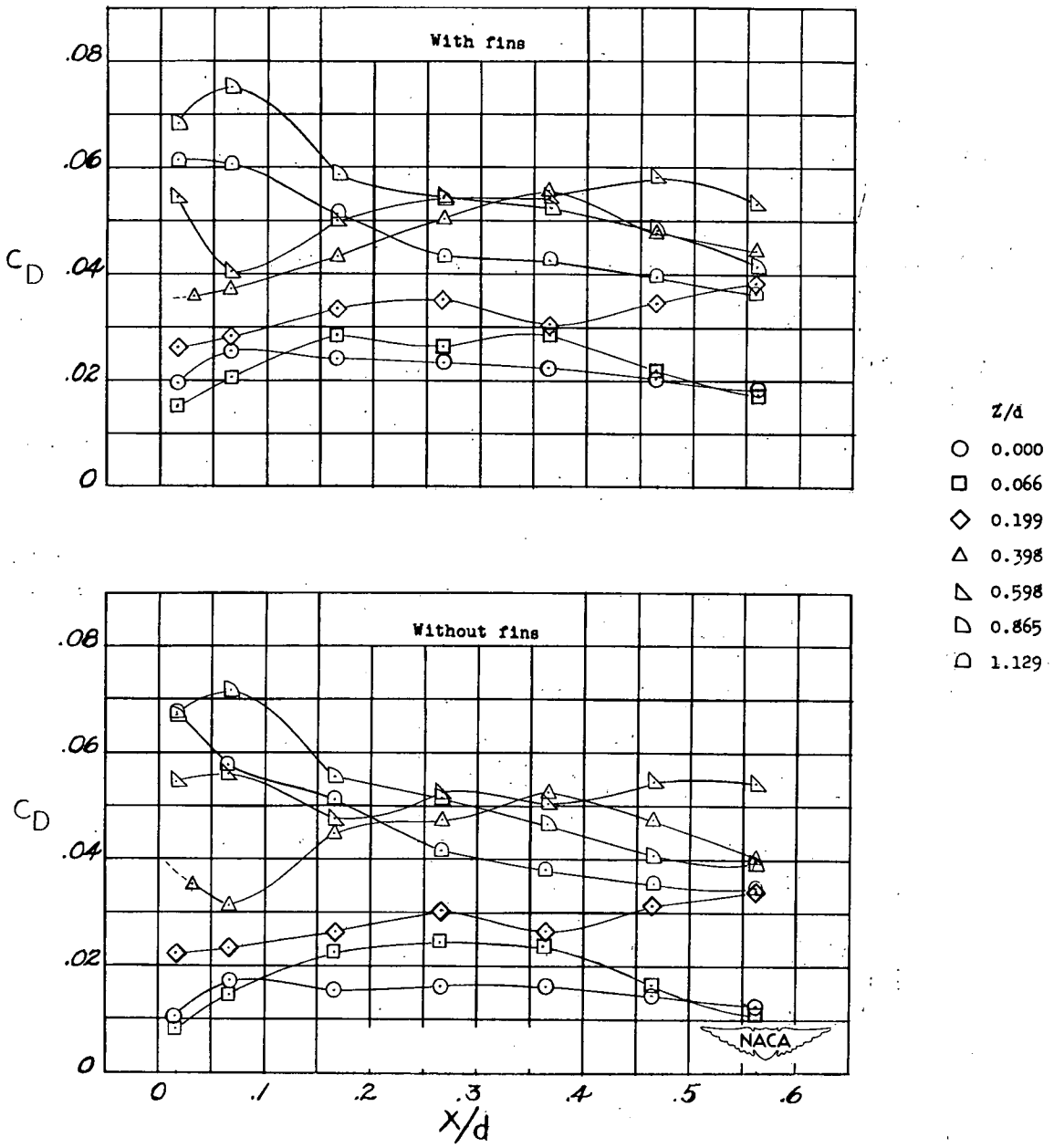

Figure 11.- Variation of C_D with X/d for various Z/d's at $\alpha = 0^{\circ}$ for model with and without fins.

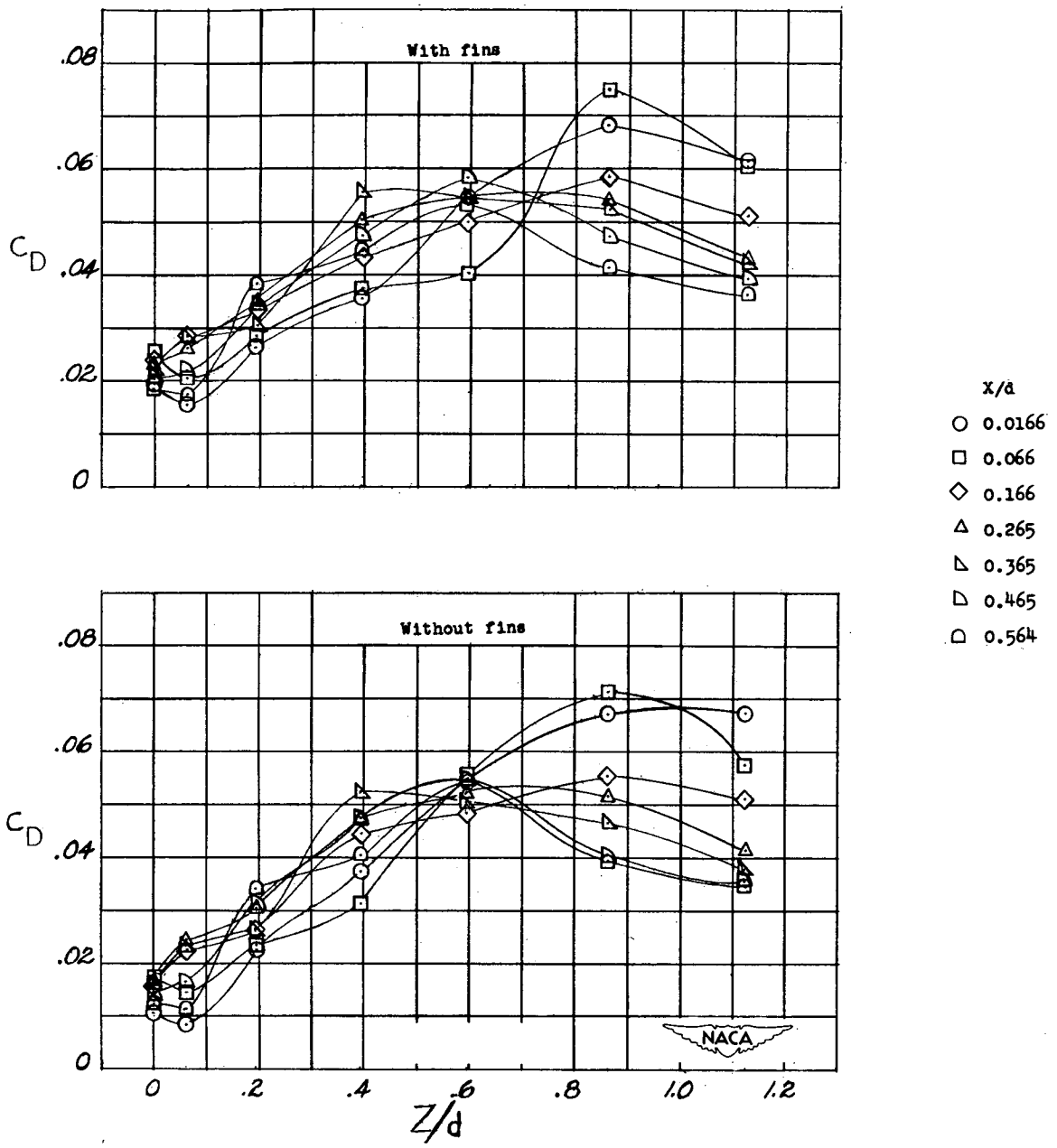

Figure 12.- Variation of C_D with Z/d for various X/d's at $\alpha = 0^{\circ}$ for model with and without fins.

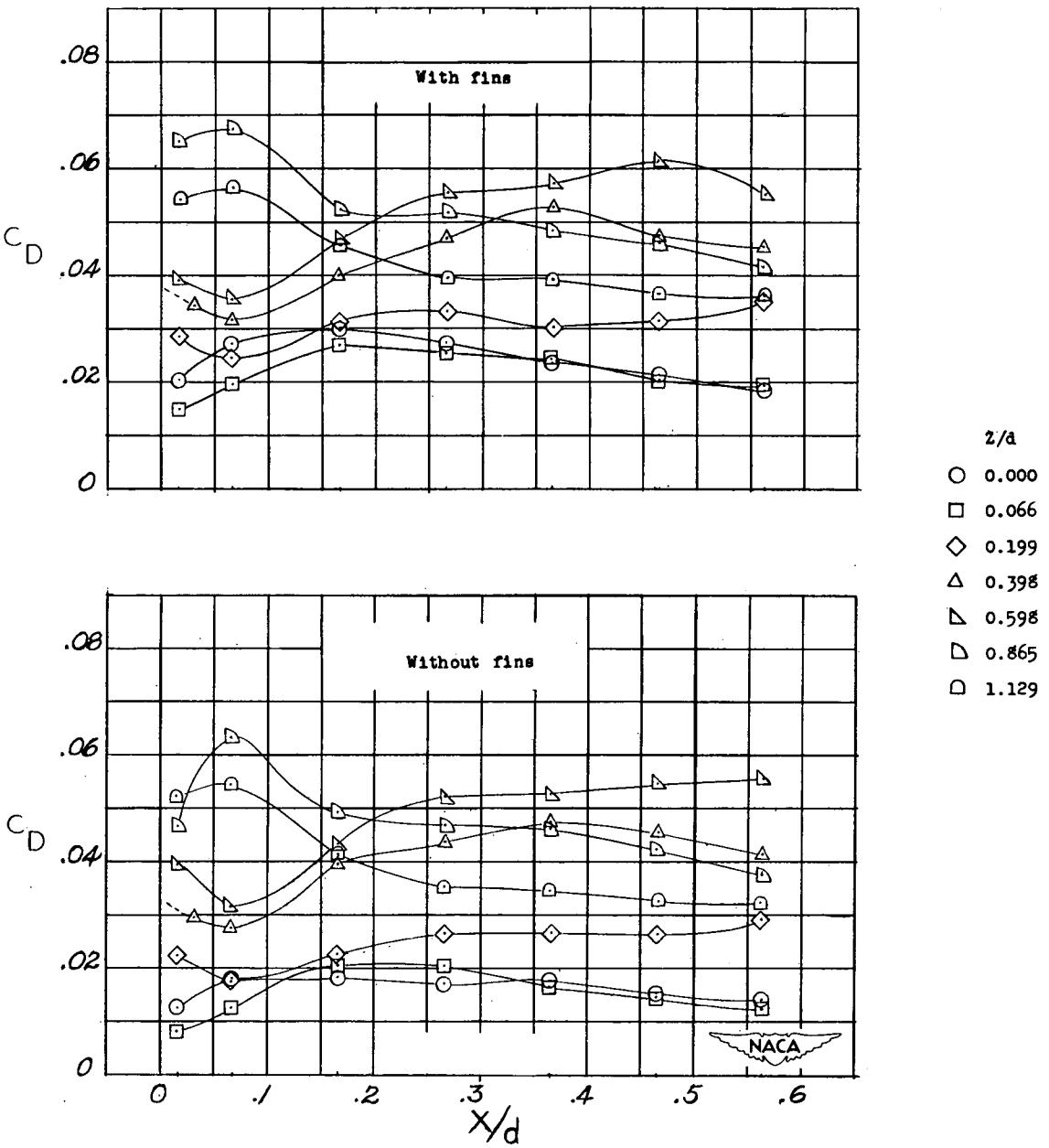

Figure 13.- Variation of C_D with X/d for various Z/d's at $\alpha = 5^{\circ}$ for model with and without fins.

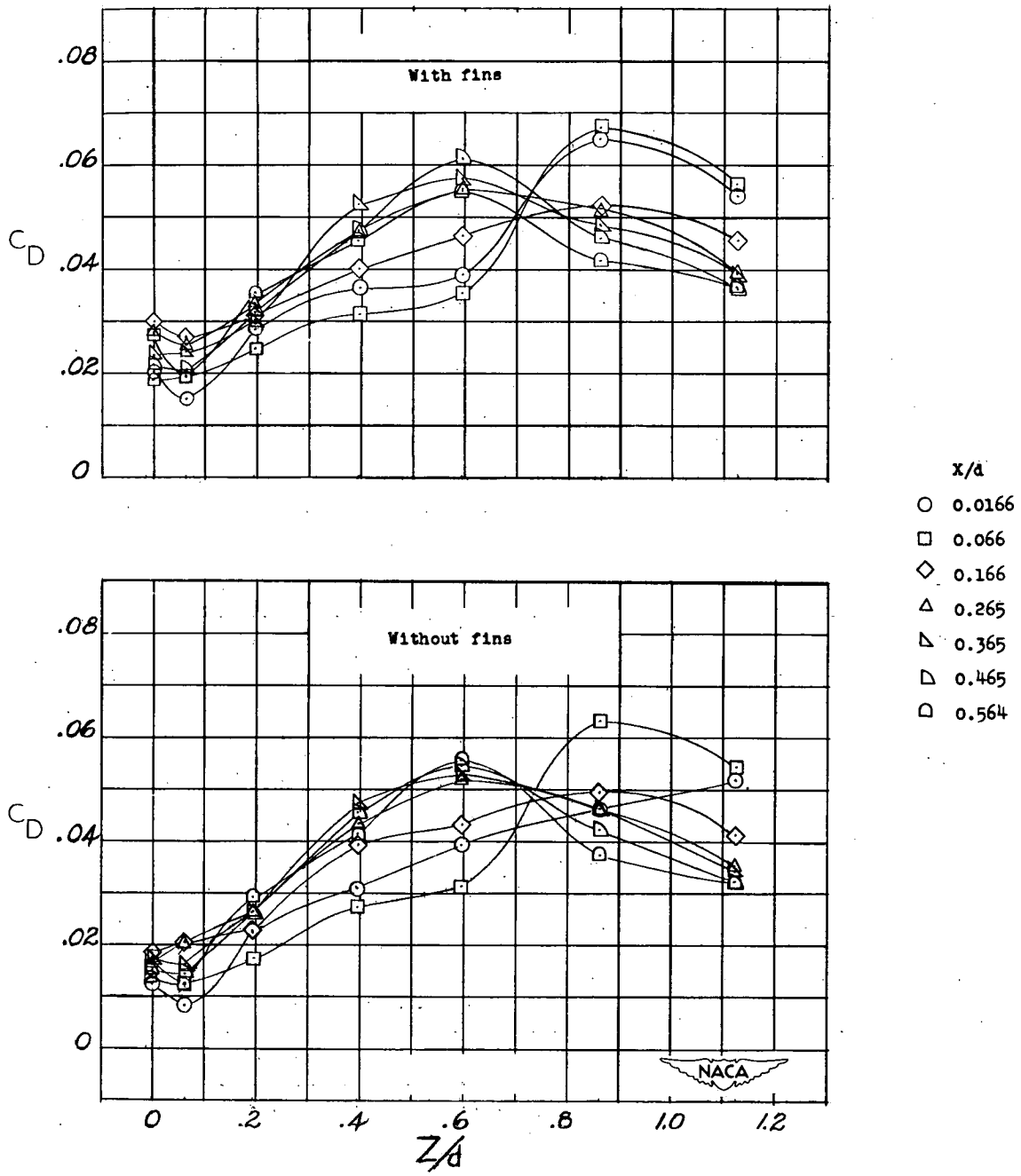

Figure 14.- Variation of C_D with Z/d for various X/d's at $\alpha = 5^{\circ}$ for model with and without fins.

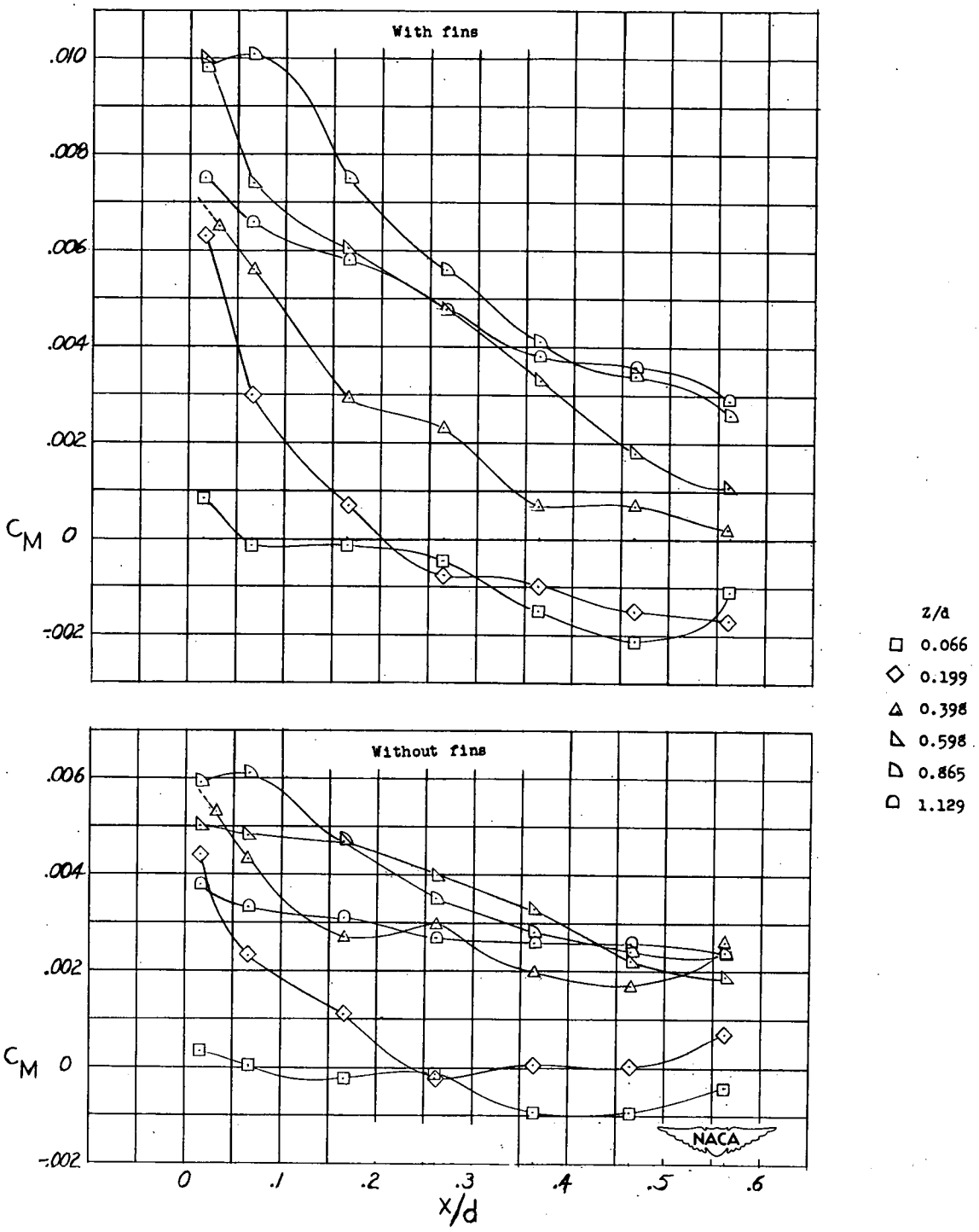

Figure 15.- Variation of C_M with X/d for various Z/d's at $\alpha = 0^{\circ}$ for model with and without fins.

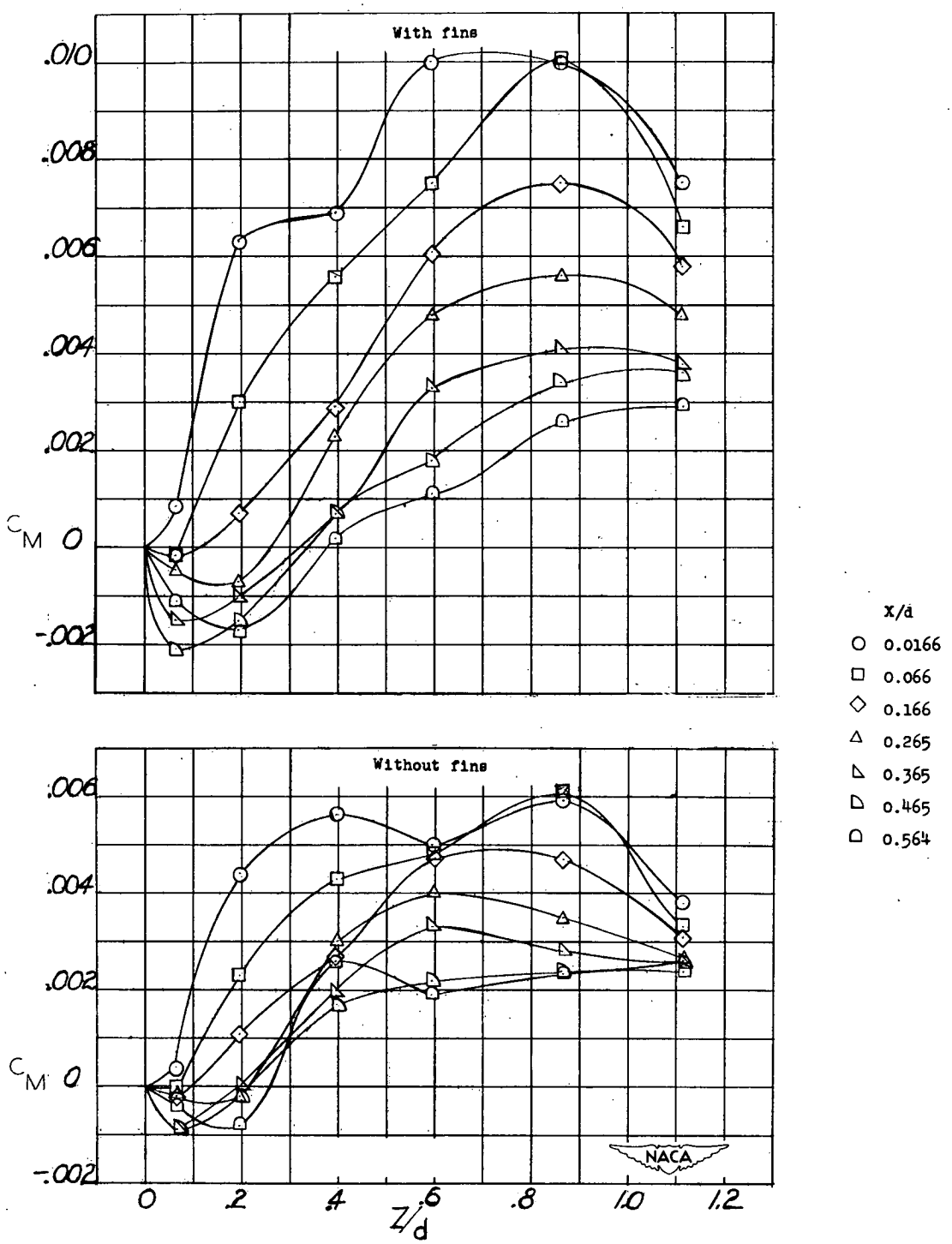

Figure 16.- Variation of C_M with Z/d for various X/d's at $\alpha = 0^{\circ}$ for model with and without fins.

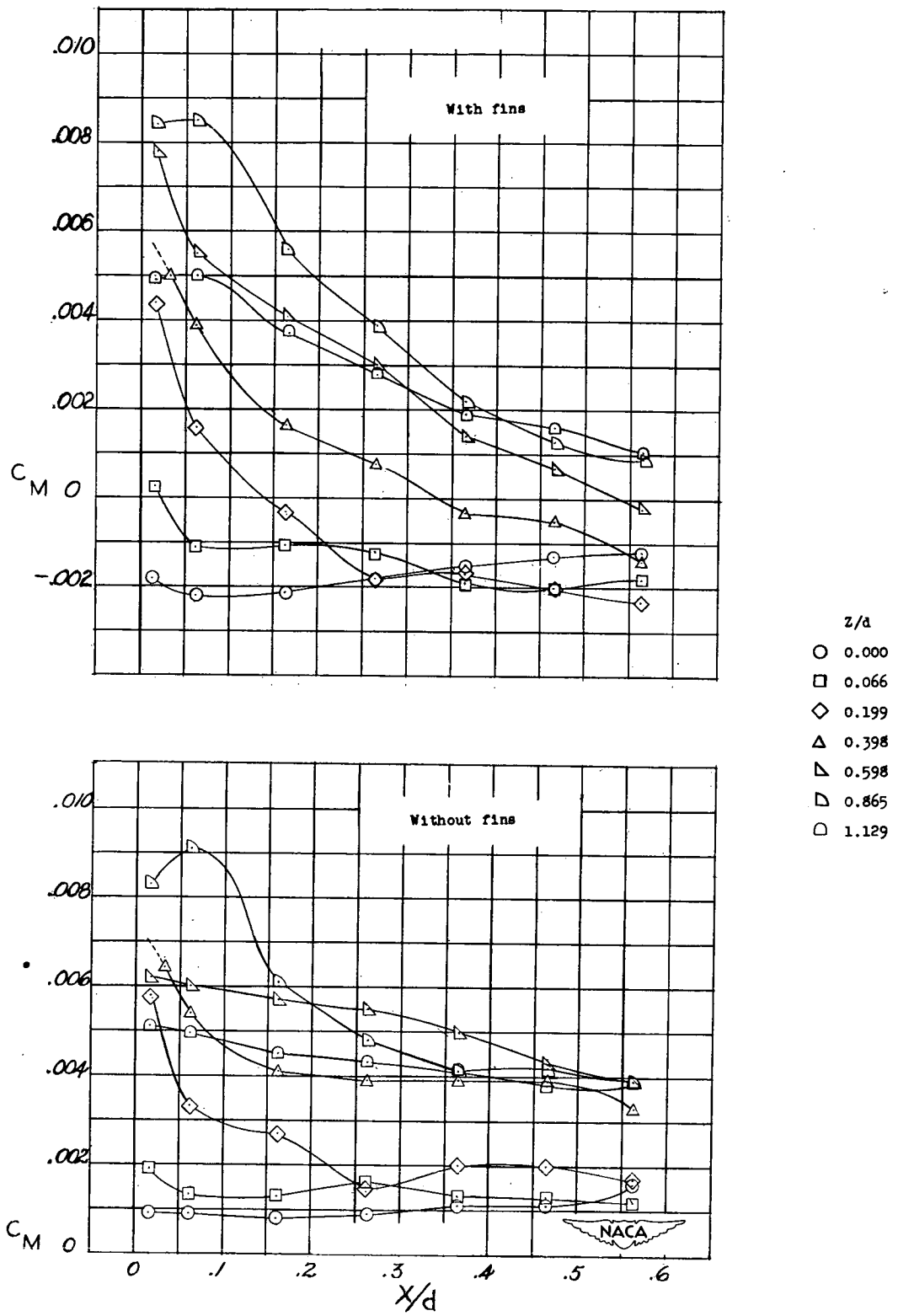

Figure 17.- Variation of C_M with X/d for various Z/d's at $\alpha = 5^{\circ}$ for model with and without fins.

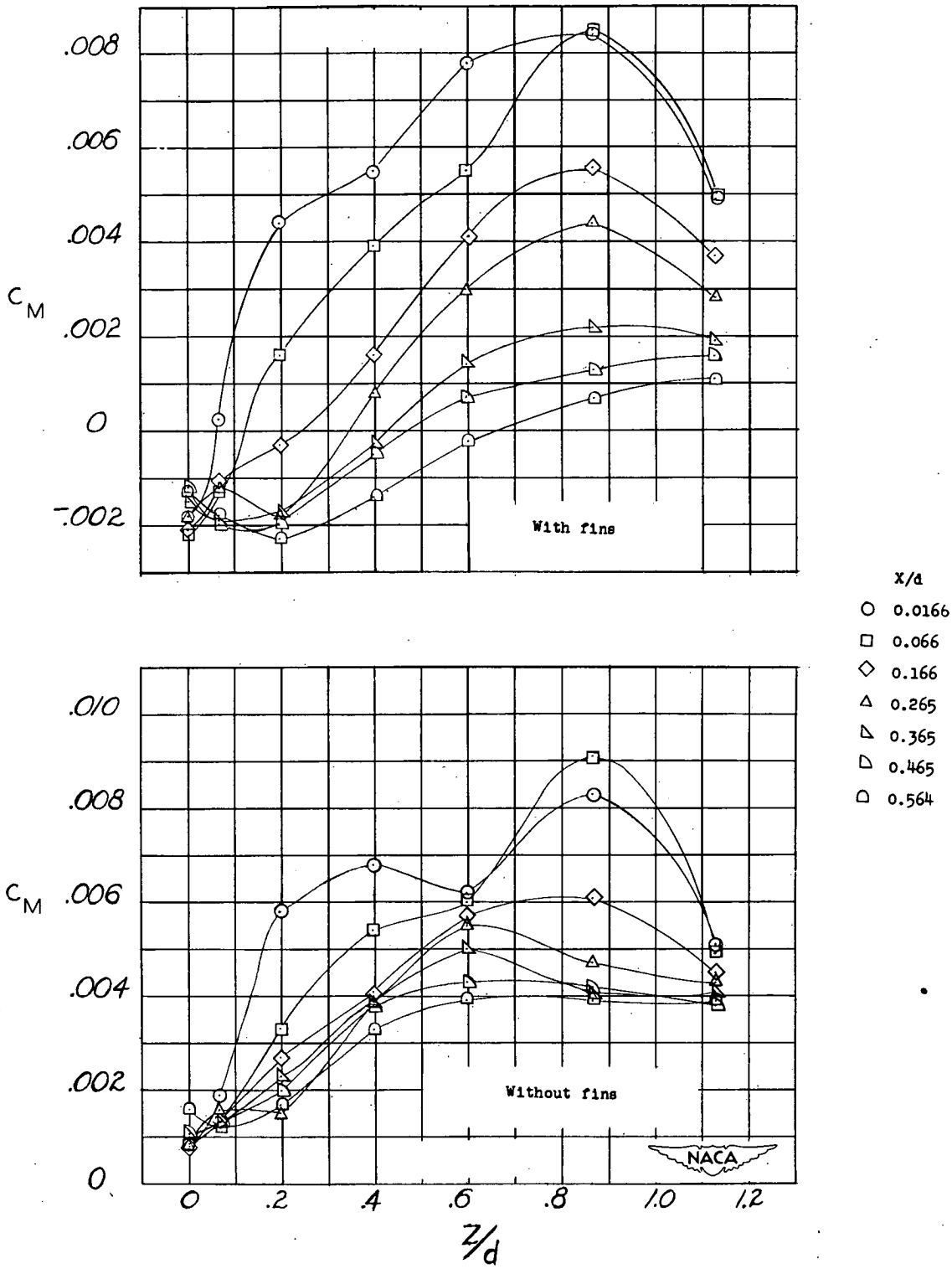

Figure 18.- Variation of C_M with Z/d for various X/d's at $\alpha = 5^{\circ}$ for model with and without fins.

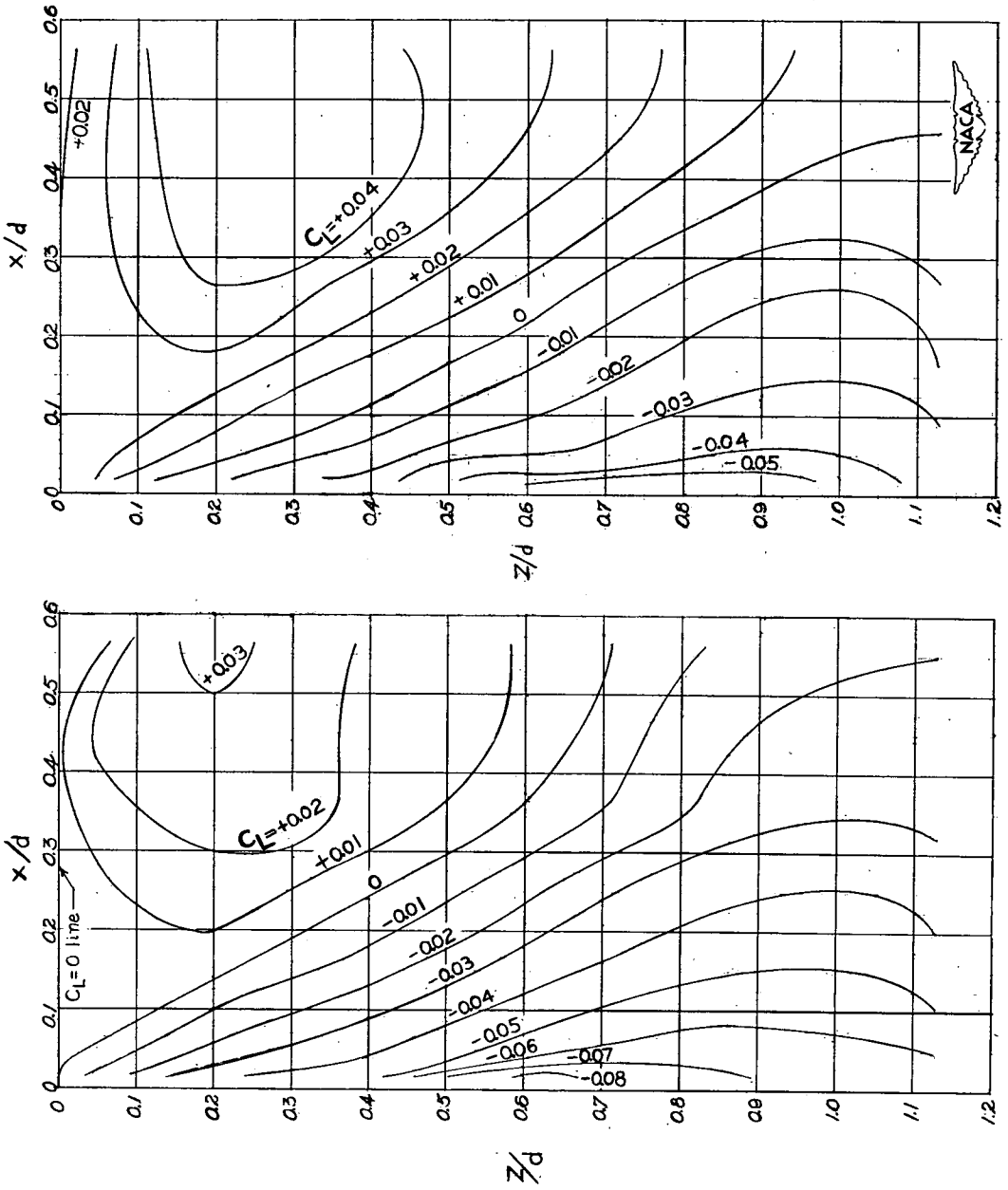

(a) $\alpha = 0^{\circ}$.

(b) $\alpha = 5^{\circ}$.

Figure 19.- Contour plot of C_L; fins installed on nose.

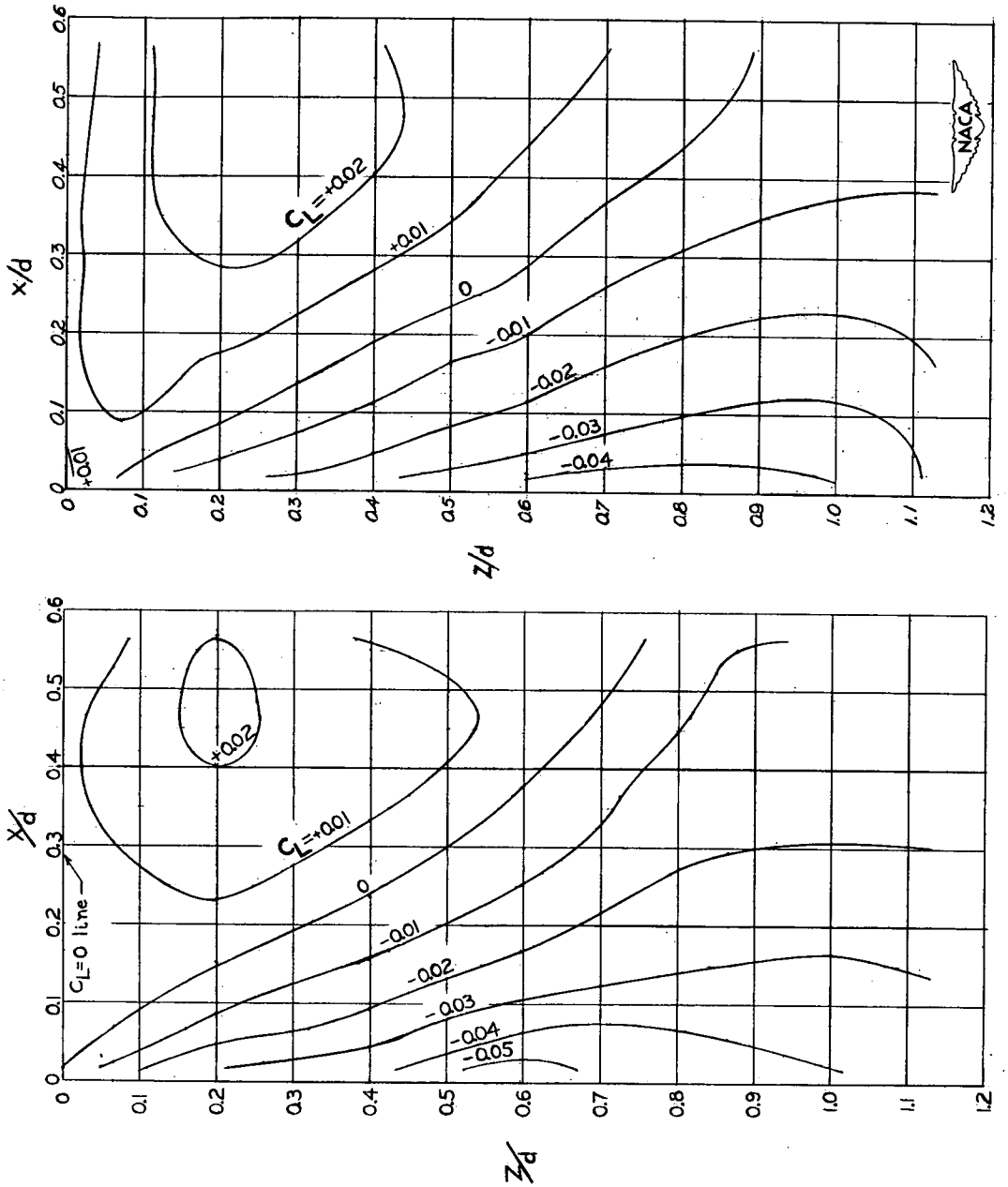

(a) $\alpha = 0^{\circ}$.

(b) $\alpha = 5^{\circ}$.

Figure 20.- Contour plot of C_L; no fins on nose.

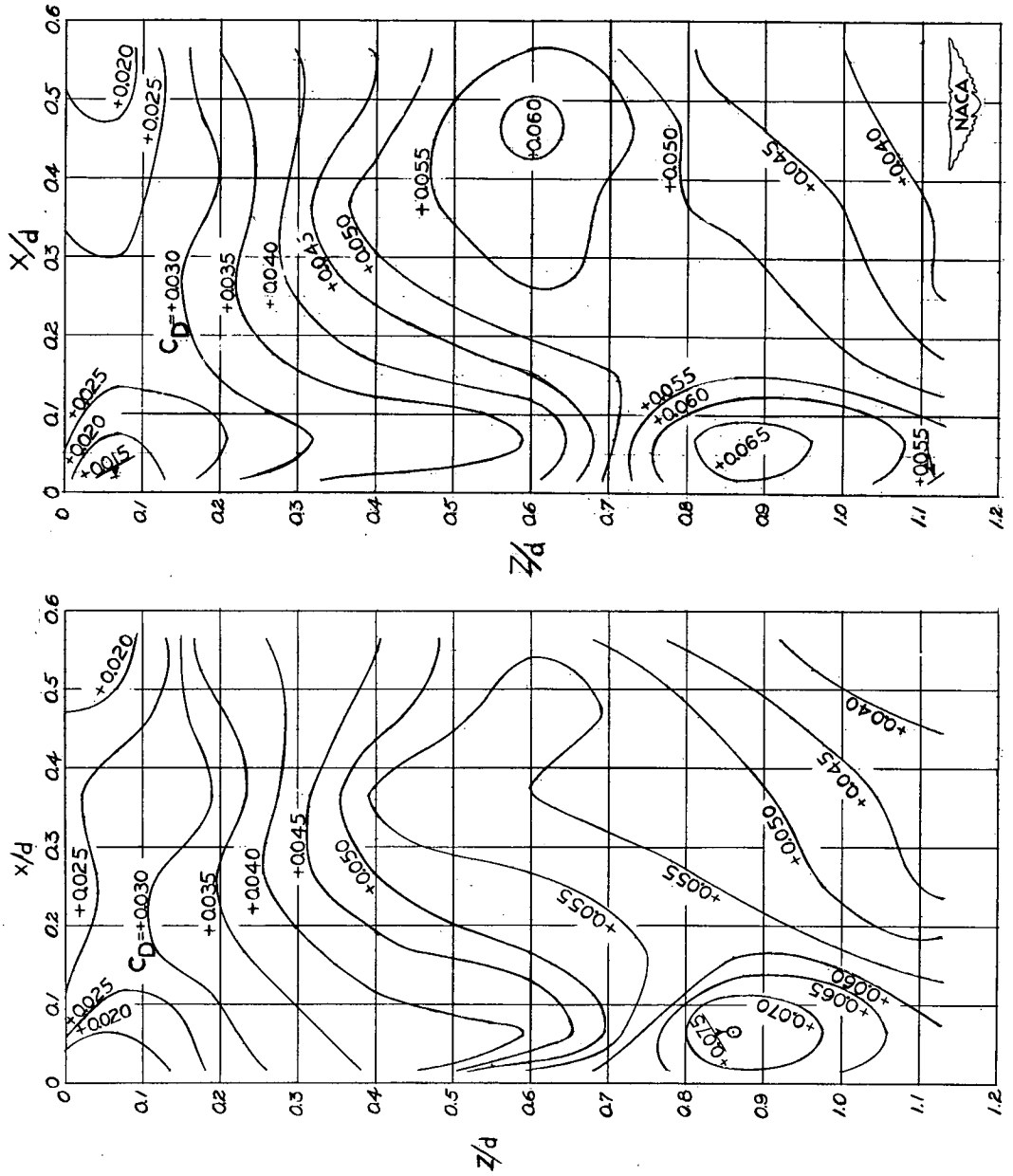

(a) $\alpha = 0^{\circ}$.

(b) $\alpha = 5^{\circ}$.

Figure 21.- Contour plot of C_D; fins installed on nose.

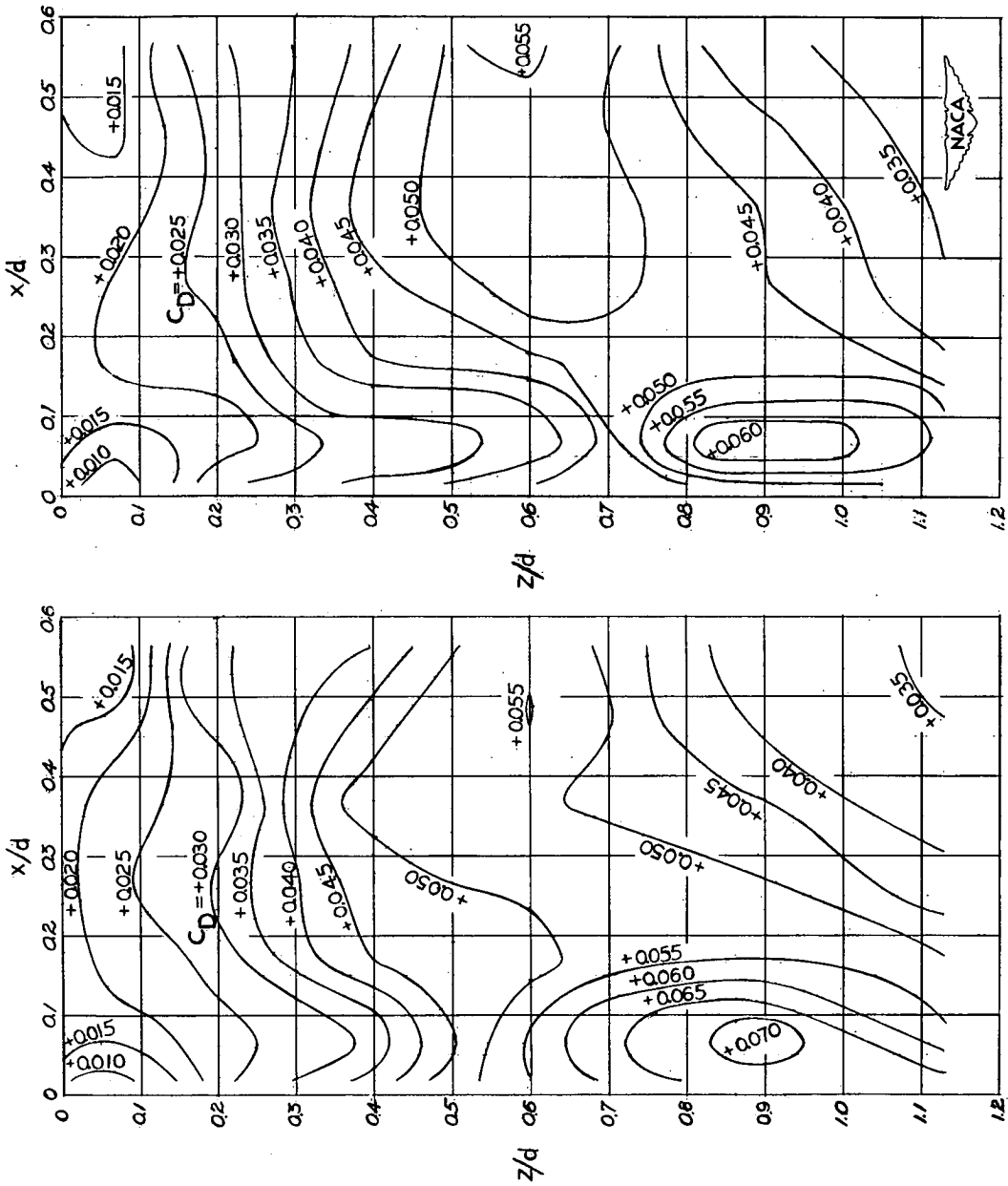

(a) $\alpha = 0^{\circ}$.

(b) $\alpha = 5^{\circ}$.

Figure 22.- Contour plot of C_D; no fins on nose.

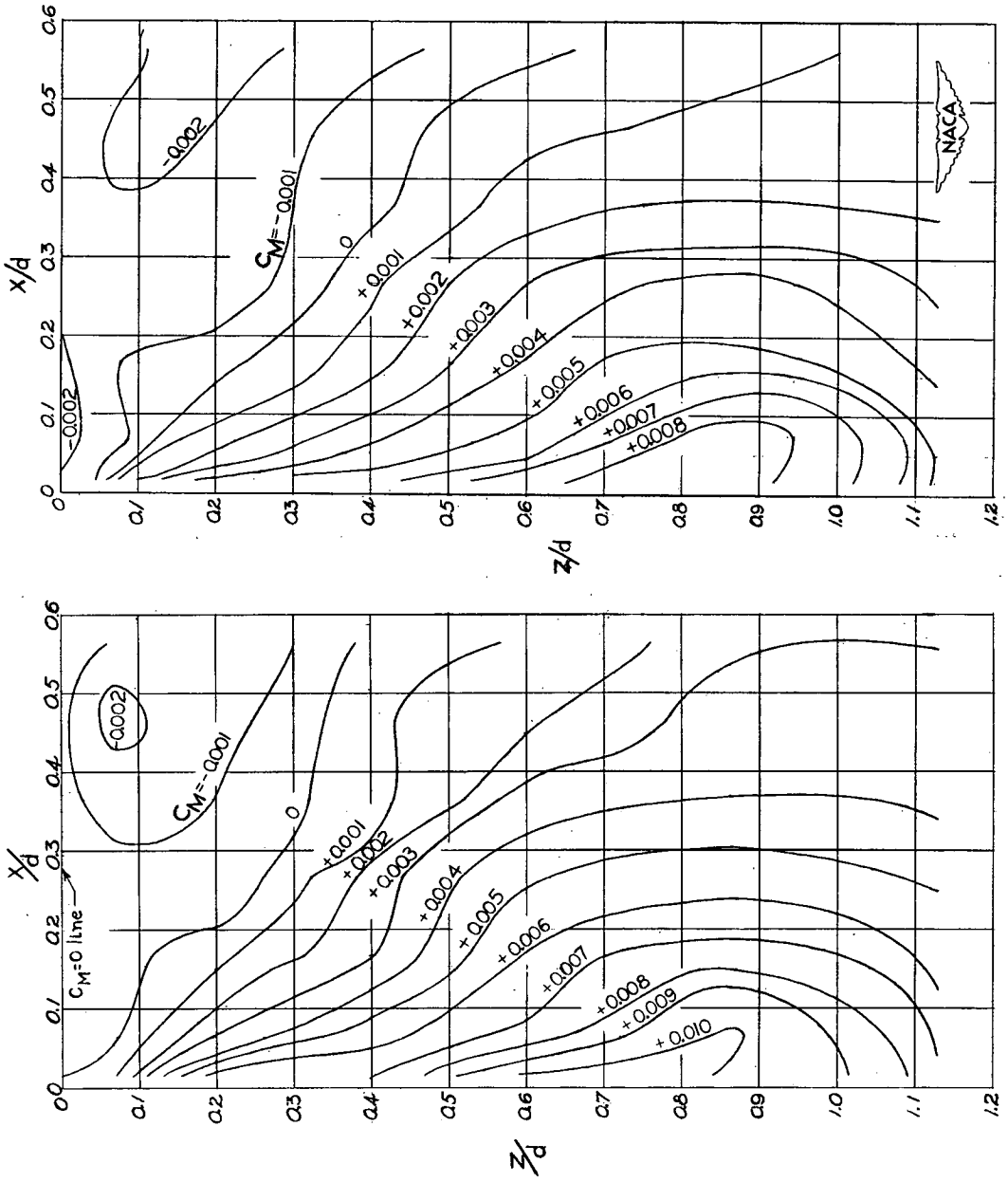

(a) $\alpha = 0^{\circ}$.

(b) $\alpha = 5^{\circ}$.

Figure 23.- Contour plot of C_M; fins installed on nose.

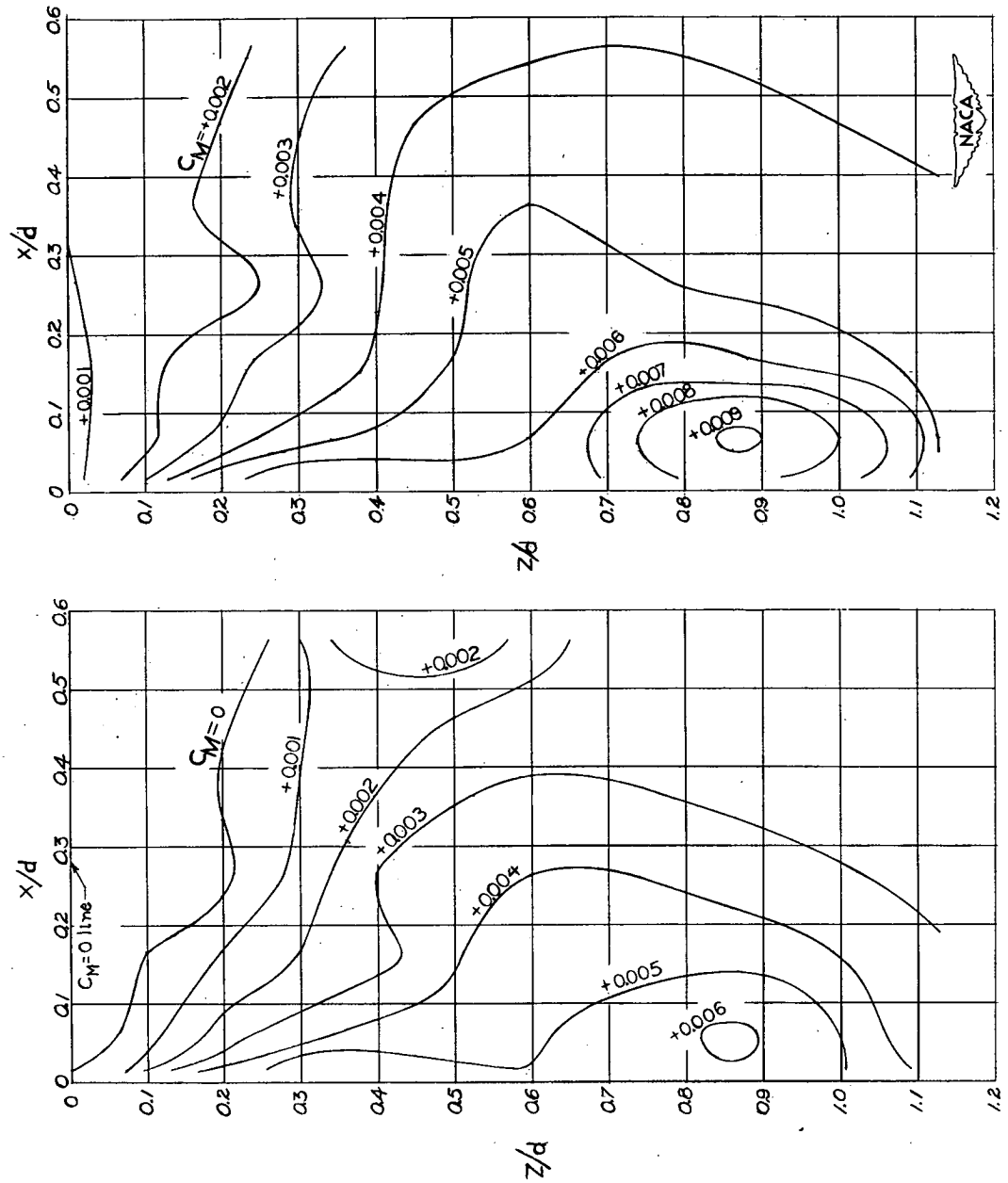

(a) $\alpha = 0^{\circ}$.

(b) $\alpha = 5^{\circ}$.

Figure 24.- Contour plot of C_M; no fins on nose.

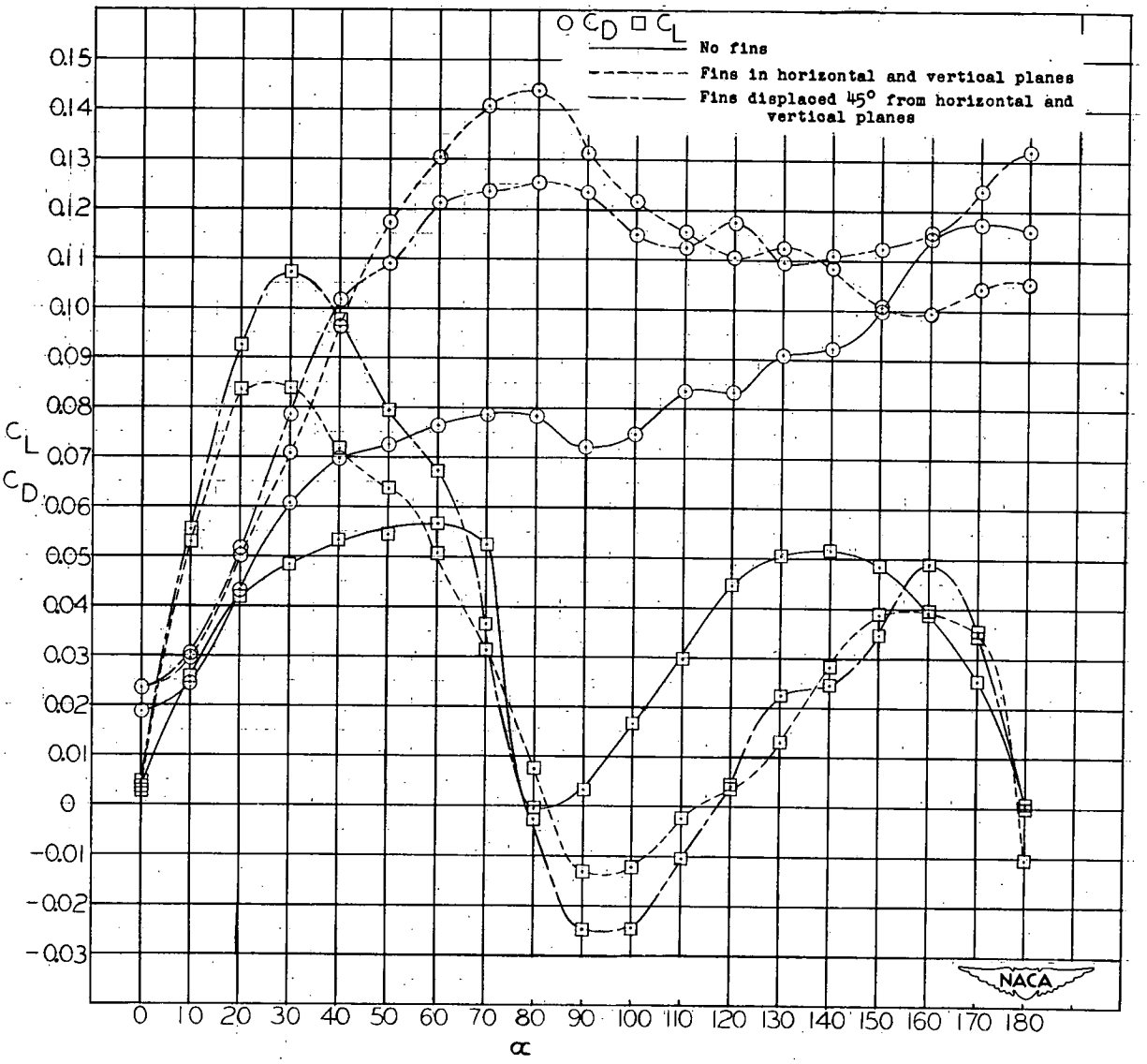

Figure 25.- Variation of C_L and C_D with α for isolated nose with and without fins.

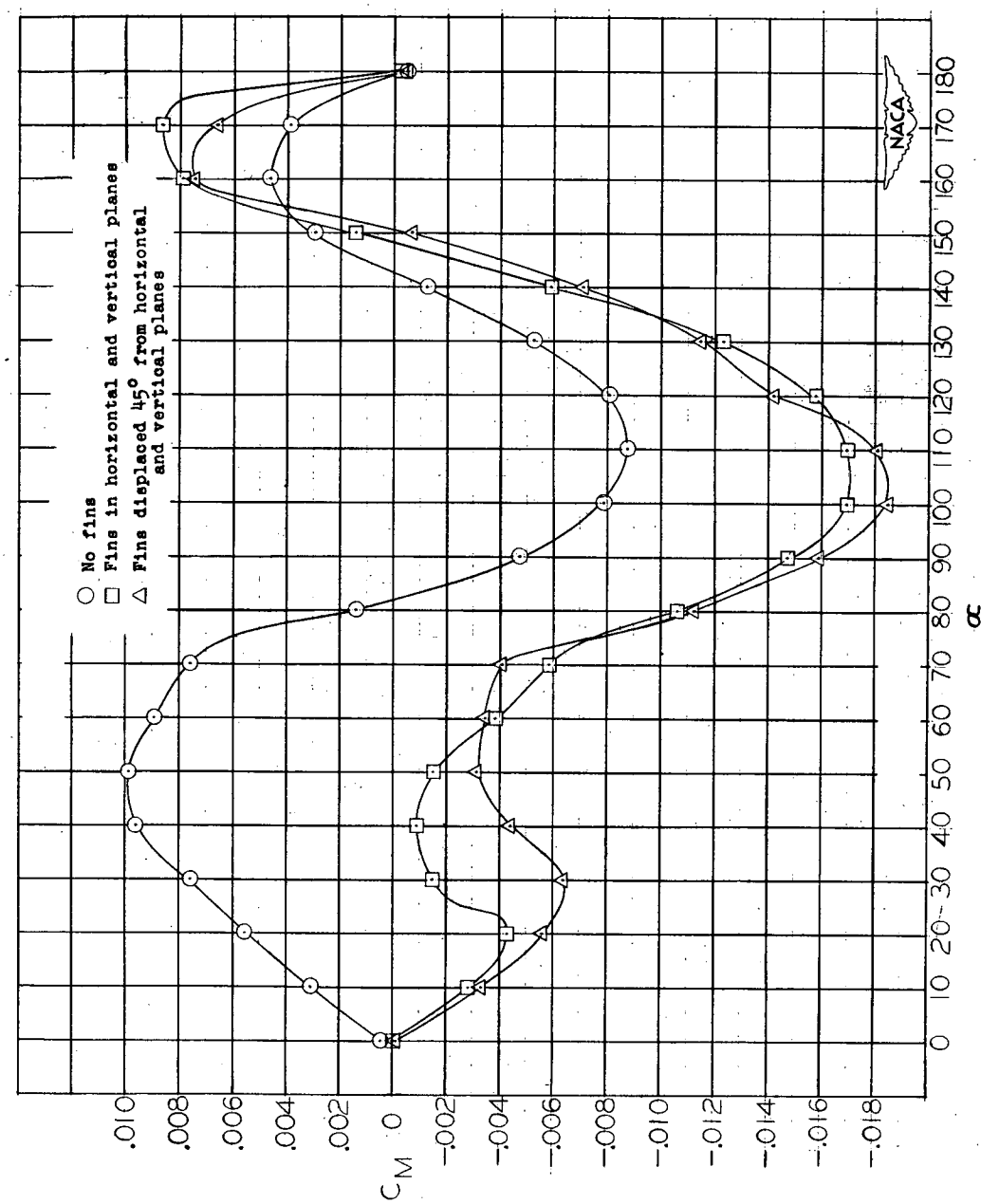

Figure 26.- Variation of C_M with α for isolated nose with and without fins.